Chapter I.13

Cyclotrons and fixed field alternating gradient accelerators

Bertrand Jacquot
Large Heavy Ion National Accelerator (GANIL), Caen, France

The cyclotrons are the most used hadron accelerators: they represent a compact and efficient solution with 100% duty cycle, very well adapted for the medical applications and for the nuclear physics research. The cyclotron maximal energy is typically 1 GeV for a proton beam. In this introductory lecture, we present the underlying concepts. The longitudinal and transverse beam dynamics in these accelerators are covered. We present specific cyclotrons (compact cyclotrons at low energy, synchrocyclotrons, "Fixed Field Alternating Gradient" accelerators, superconducting cyclotrons, separated sector cyclotrons). The concepts used in the cyclotrons are numerous, and the topic is an ideal application of many ideas introduced in a basic course in accelerator physics. We provide many exercises for a better understanding.

1 Introduction: from physics research to the medical applications

The cyclotron concept [1–4] has been developed in the years 1929–1931 by Ernest Orlando Lawrence [5]. The proposed accelerator is a generic and powerful idea: a unique acceleration radiofrequency gap crossed many times by a beam having a spiraling trajectory. Such general idea has been adapted to most of cyclic accelerators (cyclotron, synchrocyclotron, microtron, FFAG, recirculating linac).

Hence the first cyclotrons allowed the scientists to overcome the technical difficulties of the high voltage DC accelerators (Van de Graaff, Tandem). The numerous potential discoveries induced by the cyclotron idea have been recognized very soon, and a Nobel prize in Physics has been awarded to E.O. Lawrence in 1939 for his pioneering work and for the large quantity of new results obtained with cyclotrons (especially with regard to artificial radioactive elements). Then the research in nuclear and particle physics made considerable progress during the period 1930–1970 thanks to proton and ion cyclotrons. Since the 1980's, the development of facilities for the production of radionucleides used in the hospitals has opened up a new era for the cyclotrons: nowadays more than 1200 cyclotrons are in operation in the world [6]. A cyclotron can be bought on a catalog from several manufacturers (IBA, BEST, VARIAN, SIEMENS, SUMITOMO, GE, etc.). For such applications, the R&D in cyclotron is led mainly by these industrial manufacturers, which aim to reduce the cost and ease their operation in a medical context. In the near future, a larger number of cancer treatment facilities using 250 MeV proton isochronous cyclotron or synchrocyclotron could complement the standard radiotherapy. The X-rays radiotherapy uses low cost 5–15 MeV electron linac producing photons by bremstrahlung mechanism. The advantage of hadron irradiation over photon is related to the very precise tumour irradiation in a narrow range of depth, the so-called Bragg peak, minimizing radiation to the healthy nearby tissues. On

This chapter should be cited as: Cyclotrons and fixed field alternating gradient accelerators, B. Jacquot, DOI: 10.23730/CYRSP-2024-003.605, in: Proceedings of the Joint Universities Accelerator School (JUAS): Courses and exercises, E. Métral (ed.), CERN Yellow Reports: School Proceedings, CERN-2024-003, DOI: 10.23730/CYRSP-2024-003, p. 605.

the research context, the cyclotrons are very limited in their maximal energy compared to synchrotron. However many research facilities still use some very specific cyclotrons, let us cite:

- PSI (in Switzerland, providing the most powerful proton beam of 1.4 MW at 590 MeV),
- RIBF (in Japan, operating the largest superconducting cyclotron in the world),
- TRIUMF (in Canada, housing the world's largest cyclotron, which delivers H^- at 520 MeV),
- GANIL (in France, having five cyclotrons in operation).

Besides, large projects could emerge using advanced cyclotron concept for muon acceleration or accelerator driven nuclear reactor.

2 The cyclotron principle and the longitudinal dynamics

2.1 Generalities

A cyclotron consists of a very large dipolar magnet operating with a vertical magnetic field B_z generated by an electromagnet. Inside the magnet, two semicircular hollow electrodes with a D shape (called "Dees") are excited by a radiofrequency generator. A sinusoidal electric field is generated in the gap between the two cavities, (see Fig. I.13.1).

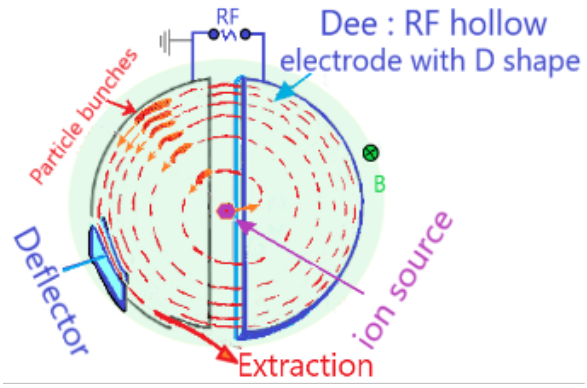

Fig. I.13.1: The cyclotron principle. The beam is injected in the centre of the cyclotron magnet from a source in the gap between the two semi-circular cavities (the "Dees").The RF voltage of the Dees produces a sinusoidal electric field in the gap. The particle bunches are accelerated after each half turn. Note that one of the Dee is at the ground potential.

The operating mode of a cyclotron is quite different from a synchrotron. The synchrotrons are pulsed accelerators: the beam is injected, then accelerated, then extracted. During the acceleration, no beam is injected into the ring, the magnet field is ramped up and the RF synchronized with beam revolution frequency. The beam is delivered to the users in pulses of a given length ΔT (typically few microseconds with a fast extraction) at a given repetition frequency F_{pulse} (usually between 1 Hz and 10 Hz). The duty cycle, i.e. the product of pulse length and repetition frequency, is very low ($< 0.01\%$), but a synchrotron can deliver beams (ions or electrons) at ultra-relativistic energy.

A cyclotron will take the continuous particle beam coming out of an ion source. The beam is bunched at a given RF frequency with a pre-buncher and then accelerated continuously. The cyclotron

delivers a continuous stream of particle bunches at RF frequency (we call it a Continuous Wave accelerator: CW). Therefore, the main advantages of the cyclotron over the synchrotron are its 100% duty cycle and its compactness (and the associated relatively low cost). However, most of cyclotron accelerators are restricted to low energy hadron beams (E $<$ 1 GeV for protons) as we will see.

In Table I.13.1 you may find a generic comparison of the characteristics of cyclotrons and synchrotrons.

Table I.13.1: Comparison of cyclotrons and synchrotrons.

	Isochronous cyclotron	Synchrotron
Revolution frequency	Constant	Variable ($\sim v$)
RF frequency	Constant cw acceleration 100% RF duty cycle	Variable: RF ramped pulsed accelerator very low RF duty cycle
Orbit radius R	Variable	Constant
Magnetic field B_z	Constant	Variable: ramped $B_{\text{dipole}} = f(\text{time}) = \frac{B\rho}{R_{\text{dipole}}}$
Transverse focusing	Weak focusing	Strong focusing with quadrupoles
Limits	Beam energy ($\gamma < 2$)	No limit in energy (except synchrotron radiation and cost)
Particles	Protons, ions	Electrons, protons, ions

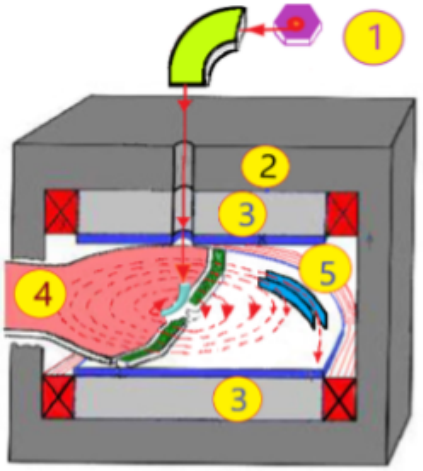

Fig. I.13.2: The "compact cyclotron" hardware. 1) External ion source: A beam line directs the beam inside the cyclotron through an axial hole, then the beam is deviated in the cyclotron plane with an electrostatic inflector. 2) The magnet yoke: One compact magnet provides the bending force to the beam. 3) The magnet poles excited by copper coils define a complex magnetic field with modulations. 4) The 180° RF Dee for acceleration: Half of the cyclotron is at the ground potential while a hollow electrode is at sinusoidal voltage. 5) An electrostatic deflector is used for beam extraction.

2.2 Revolution frequency: $\omega_{\mathrm{rev}} = qB/m\gamma$

Using a cylindrical coordinate system $(\mathbf{e_r}, \mathbf{e_z}, \mathbf{e}_\theta)$, we compute the beam revolution frequency during the acceleration in the cyclotron. A particle, having a charge q, is injected in horizontal plane of a cyclotron and the vertical magnetic field $\mathbf{B} = (0, B_z, 0)$ produces a radial force which bends the trajectories in a circular motion between each acceleration

$$\mathbf{F} = q(\mathbf{v} \times \mathbf{B}) = q(v_\theta \cdot B_z) \cdot \mathbf{e_r} \qquad . \tag{I.13.1}$$

The vector product (or "cross product") $(\mathbf{v} \times \mathbf{B})$ is not a scalar product. This vector product is computed as a matrix determinant

$$\mathbf{v} \times \mathbf{B} = \begin{vmatrix} \mathbf{e_r} & \mathbf{e_z} & \mathbf{e}_\theta \\ 0 & 0 & v_\theta \\ 0 & B_z & 0 \end{vmatrix} \qquad . \tag{I.13.2}$$

Between two successive accelerations, the relativistic Newton equation reads

$$\frac{d\mathbf{p}}{dt} = m\gamma \frac{d\mathbf{v}}{dt} = q(v_\theta \cdot B_z) \cdot \mathbf{e_r} \qquad . \tag{I.13.3}$$

The magnetic force, being always perpendicular to the particle velocity, produces an uniform circular motion. This circular motion corresponds to a radial acceleration (related to the centrifugal force, see Ex. 1).

$$\frac{d\mathbf{v}}{dt} = \left(\frac{\|\mathbf{v}\|^2}{R} \right) \cdot \mathbf{e_r} \qquad , \tag{I.13.4}$$

$$m\gamma \frac{d\mathbf{v}}{dt} = m\gamma \frac{v^2}{R} \cdot \mathbf{e_r} = q(v_\theta \cdot B_z) \cdot \mathbf{e_r} \qquad . \tag{I.13.5}$$

Rearranging the last equation, we express the radius R of the trajectory

$$R = \frac{m\,\gamma\,v_\theta}{qB_z} = \frac{\mathrm{p}}{qB_z} \qquad . \tag{I.13.6}$$

The particle revolution frequency reads

$$F_{\mathrm{rev}} = \frac{v}{2\pi R} = \frac{\mathrm{q}B_z}{2\pi m\gamma} \qquad . \tag{I.13.7}$$

Hence, in the non-relativistic approximation ($\gamma \sim 1$), the revolution frequency is independent of the energy and the beam radius in the cyclotron. We express generally the angular velocity ω_{rev}

$$\omega_{\mathrm{rev}} = \frac{d\theta}{dt} = \frac{v_\theta}{R} = 2\pi F_{\mathrm{rev}} = \frac{qB}{m\gamma} \qquad . \tag{I.13.8}$$

Exercise n^o1: Radial acceleration in circular motion

(a) Demonstrate that in a uniform circular motion, the radial acceleration is $\mathbf{a} = \frac{v^2}{R} \cdot \mathbf{e_r}$.
You can use the parametric equations for a circular motion $(X(t), Y(t))$ with:
$X(t) = R\cos(\omega t)$ and $Y(t) = R\sin(\omega t)$.

(b) Compute the velocity and the acceleration, demonstrate that the acceleration is radial.

Answer:

$v_x = \frac{dX(t)}{dt} = -\omega R\sin(\omega t)$ and $v_y = \frac{dY(t)}{dt} = +\omega R\cos(\omega t)$.
Thus, the velocity modulus is $v = \|\mathbf{v}\| = \sqrt{v_x^2 + v_y^2} = \omega R$.
Then, the acceleration is
$a_x = \frac{dv_x}{dt} = -R\omega^2\cos(\omega t)$, $a_y = \frac{dv_y}{dt} = -R\omega^2\sin(\omega t)$ and $\|\mathbf{a}\| = R\omega^2 = \frac{v^2}{R}$.
The *longitudinal velocity* $\mathbf{v}$ is perpendicular to $\mathbf{a}$ (check that $\mathbf{v}\cdot\mathbf{a} = v_x \cdot a_x + v_y \cdot a_y = 0$, so the acceleration is radial). We can conclude that, in an uniform circular motion, the acceleration vector is radial

$$\mathbf{a} = \frac{v^2}{R} \cdot \mathbf{e_r} \quad .$$

2.3 Beam synchronisation with RF

In fact, there are two alternate solutions to guarantee a proper synchronization with the RF field during the acceleration:

- Making the revolution frequency constant to match the fixed RF frequency (isochronous cyclotron),
- Matching the RF frequency to the variable revolution frequency (this is the synchrocyclotron and FFAG option, see Section 5).

We will concentrate on the isochronous technology since it provides 100% duty cycle accelerators, while the second, less used nowadays, delivers pulsed beam.

If we choose a RF generator with a constant frequency and with a voltage $V = U_0\cos(\omega_{\text{rf}} t)$, the synchronization between the beam and accelerating RF cavity requires first a careful tuning of the field B_0 at injection

$$\omega_{\text{rf}} = H(2\pi F_{\text{rev}}) = H\frac{q\,B_0}{m} \quad , \tag{I.13.9}$$

where H is an integer called the Harmonic. The early cyclotrons were designed with an uniform axial field $B_z = B_0\,\mathbf{e}_z$. If the magnetic field is uniform, the beam revolution frequency decreases progressively with energy and radius due to special relativity. Since the velocity in a circular motion is $v = \|\mathbf{v}\| = R\,\omega_{\text{rev}}$ and expressing gamma, we have

$$\omega_{\text{rev}} = \frac{qB_0}{m\gamma} = \frac{qB_0}{m}\sqrt{1 - \frac{v^2}{c^2}} = \frac{qB_0}{m}\sqrt{1 - \frac{R^2\omega_{\text{rev}}^2}{c^2}} \quad . \tag{I.13.10}$$

Hence, the ion revolution frequency decreases with the radius. The early cyclotrons, having a uniform B_z field, were not able to provide high energy beams: at large energy, because of the non-constant revolution frequency, the bunches arrive out of phase at the gap, as explained in Fig. I.13.3.

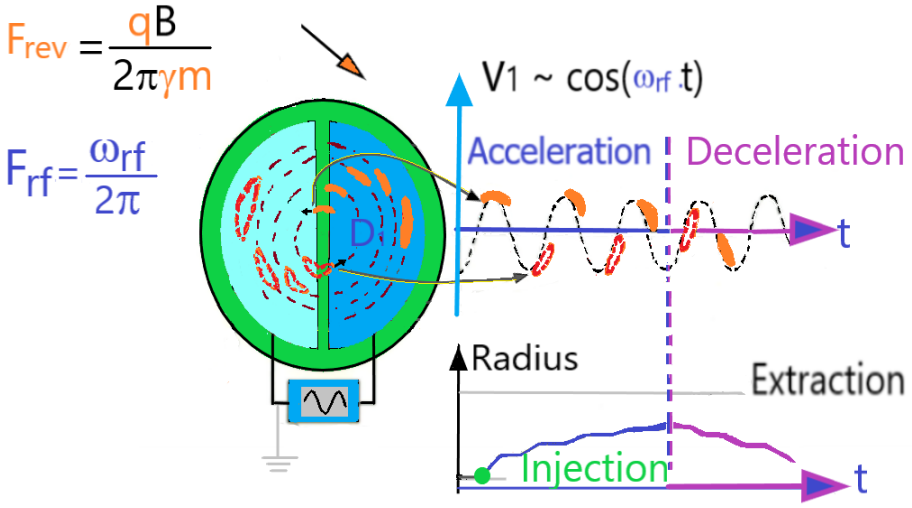

Fig. I.13.3: Desynchronization of bunches in a uniform field cyclotron. In an uniform field B_0, after a few turns when the γ factor increases the bunches arrive out of phase. Then the bunches start to be decelerated and no beam reaches the extraction. In order to maintain the acceleration the B field must vary with the radius as the Lorentz factor: $B_z = f(\text{radius}) \sim \gamma$.

2.4 Isochronous cyclotron

In order to keep the synchronisation with the RF acceleration, the vertical field B_z should follow the evolution of the relativistic γ factor. Let us choose to apply a field with the form

$$B_z(R) = B_0\, f(\text{radius}) = \frac{B_0}{\sqrt{1 - \frac{R^2\,\omega_{\text{rev}}^2}{c^2}}} \quad . \tag{I.13.11}$$

With such a field $B_z(R)$, the time for one turn is constant whatever the energy and radius

$$\omega_{\text{rev}} = \frac{q\,B_z(R)}{m}\,\frac{1}{\gamma} = \frac{q\,B_0}{m\sqrt{1 - \frac{R^2\,\omega_{\text{rev}}^2}{c^2}}}\sqrt{1 - \frac{v^2}{c^2}} = \frac{qB_0}{m} = \text{constant}. \tag{I.13.12}$$

The cyclotron is said to be ISOCHRONOUS. In Fig. I.13.4 , the bunches are shown on the RF accelerating wave for each gap crossing between the two Dees. With the isochronous condition (F_{rev} = constant), the beam arrives always at the edge of the gap at the optimum accelerating RF phase during the acceleration time.

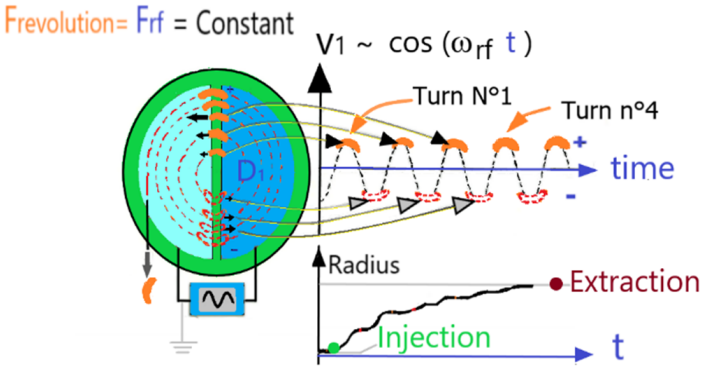

Fig. I.13.4: Bunch synchronization with RF. In an isochronous cyclotron for a perfect acceleration, the two following conditions are required:
a) Synchronism with RF at injection: $\omega_{\text{rf}} = H\,\omega_{\text{rev}} = H\,\frac{qB_0}{m}$,
b) Isochronism: ω_{rev} = constant, during the acceleration with $B_z(R) = \frac{B_0}{\sqrt{1-\frac{R^2\,\omega_{\text{rev}}^2}{c^2}}}$.

2.4.1 *Choice of RF harmonic $H = \omega_{rf}/\omega_{rev}$*

In the gap, it is required that the electric field be directed always in the right direction to obtain the acceleration. The AC generator must alternate the polarity of the 180°Dee in order to give to the ion an accelerating electric field every half period. With this cavity geometry the harmonic *H* should have an odd value (see also Section 2.5.1) Besides, the harmonic *H* will define the number of bunches per turn in the cyclotron.

2.4.2 *Variable energy cyclotron*

Most of the industrial cyclotrons for medical applications work at fixed energy. In research labs, the flexibility of the energy is important even if it requires some extra technical complexity. The ion energy variation is associated with the beam velocity at the extraction radius which imposes to modify the magnetic field and its radial dependence (to be adapted to the new γ factor), and the RF frequency.

The variable energy cyclotrons having a variable final velocity ($v_{\text{final}} = R_{\text{extraction}}\,\omega_{\text{rev}}$), requires:

- A RF cavity with variable frequency ($\omega_{\text{rf}} = H\,\omega_{\text{rev}}$) adapted for each required energy,
- A magnet with many correction coils[1] for the adjustment of the field evolution

$$B_z(R) = \frac{B_0}{\sqrt{1-\frac{R^2\,\omega_{\text{rev}}^2}{c^2}}} \quad \text{with } B_0 = \frac{\omega_{\text{rev}}\,m}{q} \quad .$$

[1]The correction coils (called trimming coils) are a set of adjustable concentric coils located on the pole pieces inside the magnet gap. Equipped with a variable frequency RF cavity and adjustable trimming coils (excited with independent power supplies), a cyclotron can accelerate a wide range of ion species (q,m) at diverse energies (γ).

Exercise n^o2: The isochronous cyclotron, numerical application

An isochronous cyclotron uses a RF cavity at 60 MHz at the RF harmonic $H = 3$

- Compute the time T_{rev} needed to perform one turn for the accelerated ions.
- Compute the average field B_0 needed to accelerate protons in a non-relativistic approximation.

Answer:

The revolution frequency is $F_{\text{rev}} = \frac{F_{\text{rf}}}{H} = 20\,\text{MHz}$. $T_{\text{rev}} = \frac{1}{20\,10^{-6}}\,\text{s} = 50\,\text{ns}$.
$\omega_{\text{rev}} = \frac{qB_0}{\gamma m} = \frac{\omega_{\text{rf}}}{H}$. At relatively low energy the Lorentz factor γ is close to 1. So, using the proton mass $m_p \sim 1.6\,10^{-27}$ kg and the proton charge $q \sim 1.6\,10^{-19}$C , we get
$F_{\text{rf}} = \frac{\omega_{\text{rf}}}{2\pi} = 60\,\text{MHz}$, so we have

$$B_0 = \omega_{\text{rev}} \frac{m_p}{q} \sim (2\pi \frac{F_{\text{rf}}}{H}) \frac{m_p}{q} = 10^{-8}\,10^6\,20\,2\pi = 1.26\,\text{T}.$$

2.5 Acceleration with RF Dees

2.5.1 The classical RF Dee with $\alpha_{cav} = 180°$

The energy gain in the accelerating gaps of the RF cavity, called "Dee", depends on the phase of the RF at the particle arrival at the gap. In an isochronous cyclotron, with constant revolution frequency, the particle's azimuth θ is connected to the revolution frequency, while the RF phase evolves like $\varphi_{\text{rf}} = H\,\theta +$ constant. With a Dee angular width $\alpha_{\text{cav}} = 180°$(see Fig. I.13.1 and I.13.2), there are two accelerations per turn. Using as a reference the phase φ_{mid} in the middle of the Dee, the phase φ_{gap1} at the entrance of the Dees

$$\varphi_{gap1} = \varphi_{\text{mid}} - \frac{H\,\alpha_{\text{cav}}}{2} \quad .$$

Remembering that the voltage should be negative at the entrance of the Dee to accelerate positive ions, if V is negative at the entrance of the Dee the energy gain δE_{gap1} at the first gap is positive

$$\delta E_{\text{gap1}} = -\,q\,V(\varphi_{\text{gap1}}) = +\,q|V(\varphi_{\text{gap1}})| \quad .$$

The energy gain per turn in the general case is

$$\begin{cases} \delta E_{\text{turn}} & = \delta E_{\text{gap1}} + \delta E_{\text{gap2}} = -qV(\varphi_{\text{gap1}}) + qV(\varphi_{\text{gap2}}) \\ & = -qU_0 \sin\left(\varphi_{\text{mid}} - \frac{H\alpha_{\text{cav}}}{2}\right) + qU_0 \sin\left(\varphi_{\text{mid}} + \frac{H\alpha_{\text{cav}}}{2}\right) \\ & = 2qU_0 \cos(\varphi_{\text{mid}}) \sin\left(\frac{H\alpha_{\text{cav}}}{2}\right) = 2qU_0 \cos(\varphi_{\text{mid}}) \sin(90°) \quad . \end{cases} \tag{I.13.13}$$

We demonstrate here that the even harmonics $H = 2, 4...$ produce no energy gain ($\sin 180° = 0$), since the energy gain in the first acceleration gap would be compensated by a deceleration in the second. In principle, all particles with a phase satisfying $-\pi/2 < \varphi_{\text{mid}} < \pi/2$, are accelerated since ($\delta E_{\text{turn}} > 0$). The particles with low energy gain are lost either at injection, extraction, or during

the acceleration. The longitudinal acceptance $\Delta\varphi$ does not exceed generally 40° (out of 360°) therefore, the optimization of the transmission requires a RF buncher upstream of the cyclotron.

2.5.2 *RF Dee with smaller angle α_{cav}*

Some cyclotrons are equipped with RF-cavities with an angular extent α_{cav} much smaller than 180°, which allows to increase the number of acceleration per turn. We present in Fig. I.13.5, a cyclotron with two independent cavities producing four accelerations per turn

$$\delta E_{\text{turn}} = N_{\text{gap}} q U_0 \sin\left(\frac{H\alpha_{\text{cav}}}{2}\right)\cos(\varphi_{\text{mid}}) \quad . \tag{I.13.14}$$

The kinetic energy of any particle after N_{turn} is connected to the phase in the cavity

$$E(N_{\text{turn}}) = E_N = E_{\text{injection}} + N_{\text{turn}}\, N_{\text{gap}}\, q\, U_0 \sin\left(\frac{H\alpha_{\text{cav}}}{2}\right)\cos(\varphi_{\text{mid}}) \quad . \tag{I.13.15}$$

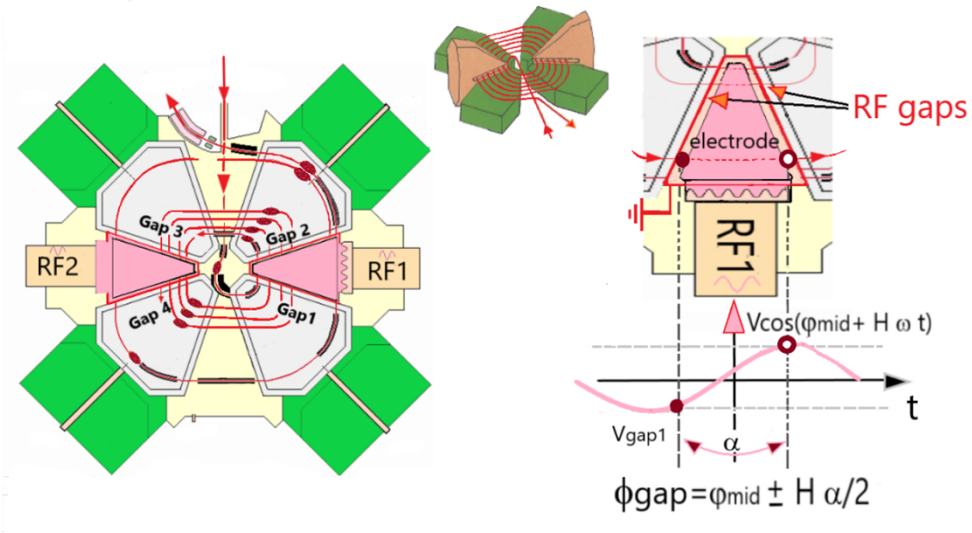

Fig. I.13.5: The Isochronous Cyclotron "SSC2" (Ganil, France). has two RF cavities with an angular width of $\alpha_{\text{cav}} = 34°$, the RF is operated with $H = 2$ (2 bunches per turn) at a frequency between 7 and 14 MHz, depending on the heavy ion beam to be accelerated. U_0 reaches 230 kVolts. The incoming beam in this cyclotron has been already pre-accelerated by 2 consecutive cyclotrons. Positive ions ($^{12}C^{6+}$, $^{40}Ca^{20+}$, ..., $^{238}U^{58+}$) are accelerated by a negative voltage at the cavity entrance, and by a positive voltage at the exit.

2.5.3 *RF acceleration, radial size ΔR and bunch separation δR*

The acceleration of a bunch having a finite length $\Delta\varphi = \omega_{\text{rf}}\,\Delta t = H\,\omega_{\text{rev}}\Delta t$, increases the bunch radial size. Two particles arriving at different times in the accelerating gap will get a different energy kick

$$\begin{cases} E_1 &= E_0 + q\,U_0\cos(0) \\ E_2 &= E_0 + q\,U_0\cos(\omega_{\text{rf}}\delta t) \end{cases} \quad . \tag{I.13.16}$$

Hence the bunch length Δt induces an energy spread which causes a radial dispersion ΔR of the bunch. The reference particle after N_{turns} is located at $R_0 = \frac{B\,\rho_0}{B_z}$.
The horizontal size of the bunch ΔR satisfies the relation [2]

$$\frac{\Delta R}{R} = \frac{\Delta B\rho}{B\rho} = \frac{\Delta p}{p} = \frac{\gamma}{\gamma+1}\frac{\Delta E_k}{E_k} \quad . \tag{I.13.17}$$

For low energy ions $\gamma \sim 1 - 1.5$ we have

$$\frac{\Delta R}{R} \approx \frac{1}{2}\frac{\Delta E_k}{E_k} \approx \frac{1}{2}\Delta\cos(\varphi) \approx \frac{1}{4}\Delta\varphi^2 \quad . \tag{I.13.18}$$

The radial beam size ΔR is very sensitive to the bunch length Δt and the harmonic H ($\Delta\varphi = H\,\omega_{\text{rev}}\,\Delta t$). Besides, the radial separation between two bunches δR, (i.e. the distance between them on two successive turns) is decreasing with the radius R in the cyclotron

$$\begin{cases} E_N &= E_{\text{injection}} + N_{\text{turn}}\,\delta E_{\text{turn}} \approx \frac{1}{2}\,m\,v^2 \approx \frac{1}{2}\,m\,(R\,\omega_{\text{rev}})^2 \\ \frac{\delta R}{R} &\approx \frac{1}{2}\,\frac{\delta E_{\text{turn}}}{E_N} \sim \frac{1}{R^2} \quad . \end{cases} \tag{I.13.19}$$

Consequently, the bunch spacing $\delta R \sim \frac{1}{R}$ is often very small at the cyclotron extraction at large radii: The bunches overlap each other and the extraction of the bunches produces beam losses on the deflector (see Section 7).

[2] In a non-relativistic approximation:

$$\frac{dE_k}{dp} = \frac{d(\frac{m\,v^2}{2})}{d(m\,v)} = \frac{d(v^2/2)}{d(v)} = \frac{2v}{2} = 2\,\frac{E_k}{p} \quad .$$

Therefore, $\frac{dp}{p} = \frac{1}{2}\,\frac{dE_k}{E_k}$, and considering relativistic mechanics, we get (see Section I.13.D)

$$\frac{dE_k}{dp} = \frac{\gamma+1}{\gamma}\,\frac{E_k}{p}.$$

Exercise n^o3: the K_b value of a cyclotron and its maximal capability

A cyclotron is designed to accelerate ions with a nucleon number A and a charge state Q.
- Demonstrate that the maximal kinetic energy ($\frac{E_k}{A}$) of a cyclotron can be written as

$$\frac{E_k}{A} = K_b \left(\frac{Q}{A}\right)^2 .$$

Note: Write the K_b factor in a non-relativistic approximation using an extraction radius R_{extr} and a magnetic field B. Assuming the ion mass is $m \sim A \cdot m_u$ and the charge Q of the ions is $q = Q \cdot e_0$. The quantity m_u is the atomic mass unit ($m_u = 1.66 \times 10^{-27}$ kg).
- A cyclotron with $K_b = 30$ MeV can accelerate protons up to 30 MeV. What would be the maximal energy of a carbon ion beam $^{12}C^{4+}$ for this cyclotron?
- What will be the revolution frequency with a field $B_0 = 1.26$ T for a proton (H^{1+}) beam and for a $^{12}C^{4+}$ beam?

Answer:

The kinetic energy is $E_k = (\gamma - 1)c^2 \simeq \frac{1}{2}mv^2$, therefore $E_k = \frac{1}{2}A\, m_u R_{\text{extr}}^2\, \omega_{\text{rev}}^2$ so,

$$\frac{E_k}{A} = \frac{1}{2} m_u R_{\text{extr}}^2 \left(\frac{Q e_0\, B}{A\, m_u}\right)^2 = K_b \left(\frac{Q}{A}\right)^2 \quad .$$

For a proton ($A = 1$, $Q = +1$), $\frac{E_k}{A} = 30\,(Q/A)^2 \ = 30\,\text{MeV}/A$.
While for $^{12}C^{4+}$ (12 nucleons, $Q = +4$), the maximal energy is
$\frac{E_k}{A} = 30\left(\frac{4}{12}\right)^2 = 3.33\,\text{MeV}/A$.
Then $F_{\text{rev}} = \frac{\omega_{\text{rev}}}{2\pi} = \frac{qB}{2\pi\, m} = 20$ MHz with protons, and $F_{\text{rev}} = 6.67$ MHz with $^{12}C^{4+}$.
Let us note that the revolution frequency for $^{12}C^{4+}$, $\omega_{\text{rev}} = \frac{q\,B}{m} \sim \frac{q\,B}{Am_u}$, is 3 times smaller than that of the proton beam. We can operate the cyclotron at $F_{\text{rf}} = 20$ MHz for the two beams, which corresponds to a harmonic number $H = \omega_{\text{rf}}/\omega_{\text{rev}} = 1$ for protons, and $H = 3$ for carbon ions. Consider also that a slight adjustment in B is needed, since the carbon ion mass is not exactly twelve times the proton mass.

3 Transverse dynamics and orbit stability

In the cyclotron magnet, the particles travel a long way before their extraction. This corresponds to many turns in the magnetic field. Therefore, it is important to study if a particle, starting with a slight deviation to the reference orbit, is transported correctly.

To study this aspect, we will introduce the following concepts: cylindrical coordinates, field index n, transverse stability, tunes, etc.

3.1 Equation of motion in cylindrical coordinates

We will provide a rigorous formulation of the particle trajectories in the vicinity of an ideal circular trajectory over one turn: we use a cylindrical coordinate system $(\mathbf{e}_r(t),\, \mathbf{e}_z,\, \mathbf{e}_\theta(t))$. An arbitrary charged

particle, evolves in the field $\mathrm{B}(\mathbf{r})$ as

$$r(t) \;=\; R\cdot\mathbf{e}_r \;+\; z\cdot\mathbf{e}_z \;=\; [R_0 \;+\; x(t)]\cdot\mathbf{e}_r \;+\; z\cdot\mathbf{e}_z \qquad . \tag{I.13.20}$$

The equations of motion are determined by: $\frac{d\mathbf{p}}{dt} \;=\; m\gamma\,\frac{d\mathbf{v}}{dt} \;=\; m\gamma\frac{d^2\mathbf{r}}{dt^2}$

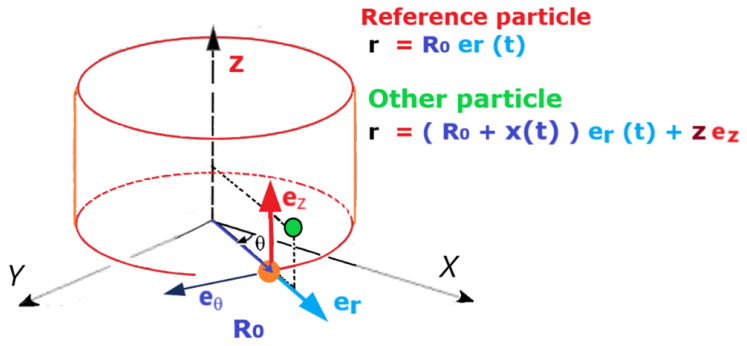

Fig. I.13.6: In the cylindrical system, the basis vector $\mathbf{e_r}$ and the azimuthal vector $\mathbf{e}_\theta$ follow the reference particle and evolve as a function of time.

The frame of reference $(\mathbf{e_r}, \mathbf{e_z}, \mathbf{e}_\theta)$ has base vectors $\mathbf{e_r} \times \mathbf{e_z} \;=\; +\mathbf{e}_\theta$. The equations of motion require the calculation of the derivative of the position vector $\mathbf{r}$. Using a Cartesian frame (X,Y), the base vectors are

$$\begin{cases} \mathbf{e}_r \;&=\; (\cos(\omega t),\, \sin(\omega t)) \\ \mathbf{e}_\theta \;&=\; (-\sin(\omega t), \cos(\omega t)). \end{cases} \tag{I.13.21}$$

Then, the vector derivatives required in the equations of motion can be written as

$$\begin{cases} \frac{d\mathbf{e}_r}{dt} \;&=\; \omega\cdot e_\theta \;=\; \frac{d\theta}{dt}\cdot\mathbf{e}_\theta \\ \frac{d\mathbf{e}_\theta}{dt} \;&=\; -\omega\cdot\mathbf{e}_r \quad . \end{cases} \tag{I.13.22}$$

Finally, we have $\frac{d^2\mathbf{e}_r}{dt^2} \;=\; -\omega^2\cdot\mathbf{e_r} = -\frac{v^2}{R^2}\cdot\mathbf{e_r}$ since $\omega = v/R$.

In the horizontal plane, the time derivatives will act on $R(t)$, $\mathbf{e}_r(t)$, and $\mathbf{e}_\theta(t)$. Since we have $\frac{d\mathbf{e}_r}{dt} \;=\; \omega\cdot\mathbf{e}_\theta \;=\; \frac{d\theta}{dt}\cdot\mathbf{e}_\theta$

$$\mathbf{v} \;=\; \frac{dr}{dt} \;=\; \frac{dR}{dt}\cdot\mathbf{e_r} \;+\; \frac{dz}{dt}\,\mathbf{e_z} \;+\; R\,\frac{d\theta}{dt}\cdot\mathbf{e}_\theta \quad . \tag{I.13.23}$$

While the acceleration $\mathbf{a}$ is determined (by using $\frac{d\mathbf{e}_\theta}{dt} \;=\; -\omega\cdot\mathbf{e_r}$)

$$\mathbf{a} \;=\; \frac{d^2r}{dt^2} \;=\; \frac{d\mathbf{v}}{dt} \;=\; \left[\frac{d^2R}{dt^2} \;-\; R\left(\frac{d\theta}{dt}\right)^2\right]\cdot\mathbf{e_r} \;+\; \frac{d^2z}{dt^2}\,\mathbf{e_z} \;+\; \left[R\,\frac{d^2\theta}{dt^2} \;+\; 2\,\frac{dR}{dt}\,\frac{d\theta}{dt}\right]\mathbf{e}_\theta \qquad . \tag{I.13.24}$$

Outside the accelerating gap, there is no electric field, the velocity modulus $\|\mathbf{v}\|$ is constant, and the Lorentz factor γ is constant: we can neglect $d\omega_{\mathrm{rev}}/dt \;=\; d^2\theta/dt^2 \;\approx\; 0$ since there is no longitudinal

acceleration. The relativistic Newton-Lorentz equation is

$$\frac{d^2\mathbf{r}}{dt^2} = \frac{q}{m\gamma}(\mathbf{v}\times\mathbf{B}) \quad . \tag{I.13.25}$$

Expressing the vector product in the cylindrical frame as a 3D determinant

$$\mathbf{v}\times\mathbf{B} = \begin{vmatrix} \mathbf{e}_r & \mathbf{e}_z & \mathbf{e}_\theta \\ v_r & v_z & v_\theta \\ B_r & B_z & B_\theta \end{vmatrix} = \mathbf{e}_r\,(v_z B_\theta - v_\theta B_z) + \mathbf{e}_z\,(-v_r B_\theta + v_\theta B_r) + \mathbf{e}_\theta\,(v_r B_z - v_z B_r) \quad . \tag{I.13.26}$$

This leads to the 3 equations used to study the stability of motion in an arbitrary field $\mathbf{B} = (B_r, B_z, B_\theta)$

$$\begin{aligned} \frac{d^2r}{dt^2}\cdot\mathbf{e_r} = \left[\frac{d^2R}{dt^2} - R\left(\frac{d\theta}{dt}\right)^2\right] &= \frac{q}{m\gamma}(v_z B_\theta - v_\theta B_z) : \text{Horizontal motion (radial)}, \\ \frac{d^2r}{dt^2}\cdot\mathbf{e_z} = \frac{d^2z}{dt^2} &= \frac{q}{m\gamma}(v_\theta B_r - v_r B_\theta) : \text{Vertical motion (axial)}, \\ \frac{d^2r}{dt^2}\cdot\mathbf{e}_\theta = R\frac{d^2\theta}{dt^2} + 2\frac{dR}{dt}\frac{d\theta}{dt} &= \frac{q}{m\gamma}(v_r B_z - v_z B_r) : \text{Longitudinal motion (azimuthal)}. \end{aligned}$$

3.2 The definition of local field index n

In an isochronous cyclotron, the magnetic field increases with the radius to fulfil the isochronism condition. As we will see later, the magnetic field will generate defocusing forces. Let's suppose that the field evolution can be described locally as a power law

$$B_z(R) = K\,R^{-n} \quad . \tag{I.13.27}$$

With the n factor called the "field index"[3] . This definition of n eases the analytical calculation of the orbit stability but does not restrict the generality. The minus sign is a convention.

The field index $n(R)$ can be seen as the fractional change in field associated with a change in radius

$$n(R) = -\frac{\left(\frac{dB_z}{B_z}\right)}{\left(\frac{dR}{R}\right)} = -\left(\frac{R}{B_z}\right)\left(\frac{dB_z}{dR}\right) \quad . \tag{I.13.28}$$

[3] **Note:** If the field is $B_z = B_0$ at $R = R_0$, the field can be written as $B_z(R) = B_0(R/R_0)^{-n}$. Around a given orbit with a radius R_0, the vertical field can be expanded at a radius $R = R_0 + x$ as

$$B_z(R = R_0 + x) = B_z(R_0) + x\left(\frac{dB_z}{dR}\right) + \cdots = B_0 - x\,n\left(\frac{B_0}{R_0}\right)\cdots = B_0\left(1 - x\frac{n}{R_0}\right) + \ldots \quad .$$

Between the poles, in the vacuum chamber, the static magnetic field satisfies $\nabla \times B = 0$. The dependence of the vertical field B_z produces a radial field component B_r as required by the Maxwell equation

$$\nabla \times B = \left(\frac{dB_\theta}{dz} - \frac{dB_z}{R\,d\theta}\right)\mathbf{e}_r + \left(\frac{d\,(R\,B_\theta)}{R\,dR} - \frac{dB_r}{d\theta}\right)\mathbf{e}_z + \left(\frac{dB_z}{dR} - \frac{dB_r}{dz}\right).\mathbf{e}_\theta \quad . \quad \text{(I.13.29)}$$

Considering that $B_z(R) = K\,R^{-n}$ and $(\nabla \times B)\cdot \mathbf{e}_\theta = 0$, we have

$$\frac{dB_r}{dz} = \frac{dB_z}{dR} = -n\,K R^{n-1} = -n\,\frac{B_0}{R} \quad , \quad \text{(I.13.30)}$$

consequently, $B_r = [-z\,n\,\frac{B_0}{R_0} + \text{ constant}]$, where the constant is zero, since $B_r(R=0) = 0$.

The radial component of $\nabla \times B$ is zero, hence $\frac{dB_\theta}{dz} = \frac{dB_z}{R\,d\theta}$, and the azimuthal component B_θ to the first order in z, is $B_\theta = z\,\frac{dB_z}{R\,d\theta} + \ldots$

For a cyclotron with a field index n [4], we expect a general magnetic field $\mathbf{B} = (B_r, B_z, B_\theta)$ with components

$$B_r = -z\,n\,\frac{B_0}{R} + \ldots \qquad B_z = \frac{B_0}{\left(1 - \frac{R^2\,\omega^2}{c^2}\right)^{1/2}} = K\,R^{-n} \qquad B_\theta = z\,\frac{dB_z}{R\,d\theta} + \ldots \quad . \quad \text{(I.13.31)}$$

[4] **Historical note on the field index**: In the early synchrotrons, the vertical focusing was not ensured by the addition of magnetic quadrupoles, but by dipoles having a slight positive field index (a decreasing field with radius: $n > 0$): this method is called *weak focusing*. In the isochronous cyclotrons, the field index is adjusted for isochronism and consequently the field has to increase with increasing energy and radius with a negative field index $n < 0$.

Exercise $n^o 4$: Field index n and γ factor

Demonstrate that in an isochronous cyclotron the field index is related to the Lorentz factor:

$$n(R) = 1 - \gamma^2.$$

- First, evaluate $\frac{dB_z}{dR}$.
- Then, remembering that $B_z(R) = KR^{-n}$ demonstrate $n = -\frac{R}{B_z}\frac{dB_z}{dR}$.

Answer:

- Since in an isochronous cyclotron $B_z = B_0\,\gamma(R)$, let's compute $\frac{dB_z}{dR} = B_0\,\frac{d\gamma}{dR}$.

$$\frac{dB_z}{dR} = B_0\,\frac{d\gamma}{dR} = B_0\,\frac{d\left(1-\frac{R^2\omega^2}{c^2}\right)^{-1/2}}{dR} = B_0\left(-\frac{2R\omega^2}{c^2}\right)\cdot(\frac{-1}{2})\cdot\left(1-\frac{R^2\omega^2}{c^2}\right)^{-3/2}.$$

So the derivative of the field appears as

$$\frac{dB_z}{dR} = B_0\left(\frac{\beta^2}{R}\right)\left(1-\frac{R^2\omega^2}{c^2}\right)^{-3/2} = \frac{B_0}{R}\beta^2\gamma^3 = \frac{B_0\gamma}{R}\beta^2\gamma^2 = \left(\frac{B_z}{R}\right)\beta^2\gamma^2.$$

Remembering that $\gamma^2 = \frac{1}{1-\beta^2}$ implies that $\beta^2\gamma^2 = \gamma^2 - 1$ (see Section I.13.D). Thus

$$\frac{dB_z}{dR} = \frac{B_z}{R}\beta^2\gamma^2 = -\left(\frac{B_z}{R}\right)\left(1-\gamma^2\right).$$

- Besides,the field derivative is connected to n

$$\frac{dB_z}{dR} = -n\,K\,R^{-n-1} = -n\,\frac{B_z}{R}.$$

- By identification of two last expressions, we get the field index n

$$n(R) = 1 - \gamma^2(R).$$

In an isochronous cyclotron, n is negative. So, the magnetic field $B_z(R)$ has to increase with radius, when γ increases with the acceleration.

3.3 Horizontal stability and the radial tune

A reference particle (m, q, $\mathbf{v} = v_0\,\mathbf{e}_\theta$) is injected in a cyclotron having a field $B_z(R) = B_0\left(\frac{R}{R_0}\right)^{-n}$ at a radius $R = R_0$. The field B_0 is adjusted to $B_0 = \frac{(p_0/q)}{R_0} = \frac{B_\rho}{R_0}$. The trajectory of such a particle describes a perfect circle of radius $R = \frac{B_\rho}{B_z} = R_0$ which corresponds to the radius of injection. If a particle with the same velocity $v_0 = R_0, \omega$ is injected a radius $R = R_0 + x$, it will oscillate around the ideal trajectory.

The projection of the Newton equation on an horizontal plane (the radial plane), as shown gives (see Section 3.1)

$$\frac{d^2\mathbf{r}}{dt^2}\cdot\mathbf{e_r} = \left[\frac{d^2R}{dt^2} - R\left(\frac{d\theta}{dt}\right)^2\right] = \frac{d^2R}{dt^2} - R\omega^2 = \left[\frac{d^2R}{dt^2} - R\left(\frac{v_0}{R}\right)^2\right] = \frac{q}{m\gamma}(v_z\,B_\theta - v_\theta\,B_z) \quad . \tag{I.13.32}$$

Substituting for this particle $\frac{d\theta}{dt} = \omega = v/R = v_0\,/\,R$ and $R = R_0 + x$ we have

$$\left[\frac{d^2x}{dt^2} - \frac{{v_0}^2}{R_0 + x}\right] = \frac{q}{m\gamma}(v_z\,B_\theta - v_\theta\,B_z) \quad . \tag{I.13.33}$$

And since to the first order in x

$$(R_0 + x)^{-1} = R_0^{-1}\,(1 + x/R_0)^{-1} = R_0^{-1}\,(1 - \frac{x}{R_0} + 0(x^2)) \tag{I.13.34}$$

we obtain

$$\left[\frac{d^2x}{dt^2} - \omega^2\,R_0\,(1 - x/R_0 + \dots)\right] = \frac{q}{m\gamma}\,(v_z\,B_\theta - v_\theta\,B_z) \quad . \tag{I.13.35}$$

In our case, with no azimuthal component of the magnetic field, $(v_z\,B_\theta)$ is zero since $B_\theta = 0$:

- The particle velocity is $v_\theta = v_0 = R_0\,\omega$ and $q\,B_0/m\gamma = \omega$,
- The field around R_0 is $B_z = B_0(1 - x\,\frac{n}{R_0}) + 0(x^2)$

$$\left[\frac{d^2x}{dt^2} - \omega^2\,R_0\,(1 - x/R_0) + \dots\right] = -\frac{q}{m\gamma}v_\theta B_z = \frac{q\,B_0}{m\gamma}[R_0\,\omega]\,[-x\,\frac{n}{R_0} + \dots] \quad . \tag{I.13.36}$$

Rewriting the equation, we obtain

$$\frac{d^2x}{dt^2} = -\omega^2\,(1 - n)\,x + \dots \quad . \tag{I.13.37}$$

The field index n, being negative in an isochronous cyclotron since $\frac{dB_z}{dR} > 0$, the quantity $(1 - n)$ is positive suggesting a sinus like solution for the differential equation. A particular solution can be found using the initial condition $x(t = 0) = x_0$. At the first order, we get

$$x(t) = x_0\,\cos(\omega\,Q_r\,t + \phi) \quad \text{with} \quad Q_r = (1 - n)^{1/2} \quad . \tag{I.13.38}$$

The quantity $Q_r = (1 - n)^{1/2}$ is called the "radial tune", and it corresponds to the number of oscillations per turn in the radial plane around the reference orbit. This motion is a stable oscillation.

3.4 Vertical stability

Let us follow a particle starting at radius $R = R_0$ at a position $z = z_0$ between the poles. The study of the motion is obtained by projecting the Newton equation on the $\mathbf{e_z}$ axis, see Section 3.1

$$\frac{d^2\mathbf{r}}{dt^2} \cdot \mathbf{e_z} = \frac{d^2 z}{dt^2} = \frac{q}{m\gamma}(v_\theta B_r - v_r B_\theta) \quad . \tag{I.13.39}$$

Using $\nabla \times B = 0$, the field index produces a radial component $B_r = -n B_0 z/R$, while the angular component derives from an angular modulation of $B_\theta = z \frac{dB_z}{R\, d\theta} + \ldots$

The revolution frequency being $\omega = \frac{q B_0}{m\gamma}$ to the first order in z

$$\frac{d^2 z}{dt^2} = \frac{q}{m\gamma}\left(-R\,\omega\, n \frac{B_0\, z}{R} - v_r\, z \frac{dB_z}{R\, d\theta}\right) = -\omega^2 \left(n + \frac{v_r}{\omega\, B_0}\frac{dB_z}{R d\theta}\right) z = -\omega^2 Q_z^2 z \quad . \tag{I.13.40}$$

The quantity called "vertical tune" Q_z is defined as

$$Q_z^2 = \left(n + \frac{v_r}{\omega\, B_0}\, \frac{dB_z}{R\, d\theta}\right) \quad . \tag{I.13.41}$$

The nature of the dynamics in the vertical plane will depend on the sign of Q_z^2:

- When $Q_z^2 < 0$: vertical instability
  If the azimuthal component of the field is zero $B_\theta = 0$, $Q_z^2 = n$ since $\frac{dB_z}{d\theta} = 0$. A particular solution of the equation is an exponential: the field index is negative in isochronous cyclotron (see ex. n°4, $n = 1 - \gamma^2$)

  $$z(t) = z_0 \exp\left(\omega \mid -n\right|^{1/2} t) = z_0 \exp\left(\mid -n\right|^{1/2} \theta) \quad . \tag{I.13.42}$$

  All the trajectories with $z_0 \neq 0$ will diverge exponentially (the particle transmission of such a cyclotron would be very low, the vertical acceptance being very small).
- When $Q_z^2 > 0$: vertical stability
  With some angular modulations on the magnet poles providing a non zero B_θ component, the quantity Q_z^2 can become positive: $Q_z^2 = \left(n + \frac{v_r}{\omega\, B_0}\, \frac{dB_z}{R\, d\theta}\right) > 0$. A particular solution of the equation is a cosine

  $$z(t) = z_0 \cos\left(\omega\, Q_z\, t + \phi\right) \text{ with } Q_z = \sqrt{\left(n + \frac{v_r}{\omega\, B_0}\, \frac{dB_z}{R\, d\theta}\right)} \quad . \tag{I.13.43}$$

The quantity Q_z corresponds to the number of oscillations per turn of any particle around the reference orbit in the vertical plane. The angular field modulation $B_z = B_0\, F(R, \theta)$ associated with the B_θ component is used to provide additional vertical focusing. Cyclotrons with such field dependence are called “Azimuthally Varying Field Cyclotron” and have a much larger particle transmission.

3.5 Qualitative understanding of the vertical instability

In the isochronous cyclotrons, the vertical field B_z should increase with the radius such to compensate the increase of the γ factor and to keep ω_{rev} constant. This can be obtained by using correction coils or, by reducing the gap at large radius (since the local field B_z is inversely proportional to the aperture

between the two poles: $B_z(R) \sim 1/R_{\text{gap}}$.

The non-uniformity of the magnetic field B_z generates a radial field component B_r (see Fig. I.13.7).

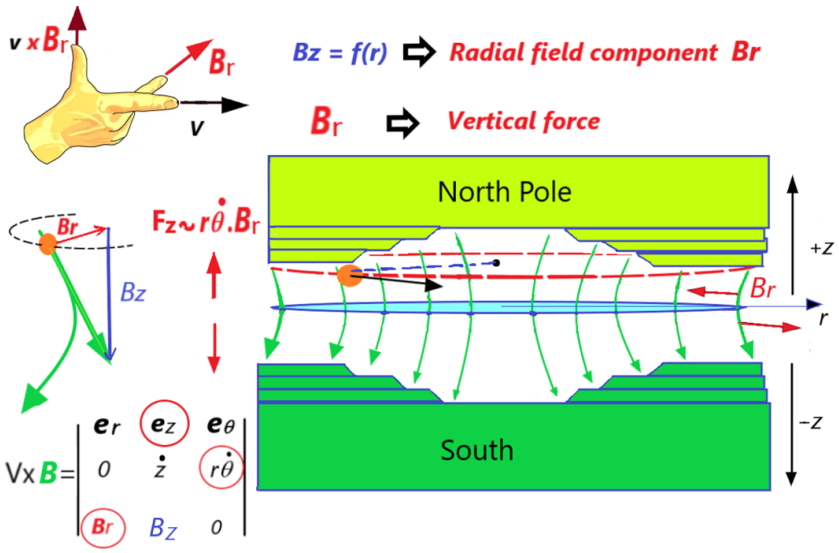

Fig. I.13.7: An increasing field at large radius, obtained with non uniform gap $g \sim 1/R_{\text{gap}}$, generates vertical defocusing forces. The magnetic field lines are perpendicular to the pole surfaces due to the Maxwell equation ($\nabla \times B = 0$). The curvature of the magnetic field lines depicted corresponds to a radial component B_r .

We see on Fig. I.13.7 that the increasing field $B_z(R)$ generates a radial field whose sign is connected to the sign of z: $B_r = -\, n\, B_0 \frac{z}{R}$

- In the upper plane, B_r is directed to the centre of the cyclotron magnet and this generates a vertical force F_z toward the top, as it can be seen with the right hand rule: $F_z = q(\mathbf{v} \times \mathbf{B}) \cdot \mathbf{e_z} = q\, v_\theta\, B_r \propto +z$;
- In the lower plane, B_r is directed outwards, generating a vertical force F_z directed downward;
- In the median plane, $B_r = 0$ because of the symmetry, and no vertical force is generated on a moving charged particle.

Hence, the requirement of increasing field $B_z(R)$ produces a this vertical defocusing force in all isochronous cyclotron. As a consequence, the particles that are not injected exactly on the median plane $(z = 0)$ could hit the cyclotron pole.

The solution to overcome the defocusing force in isochronous cyclotron will be to add an azimuthal field component B_θ , as we will see in Section 4.

4 Azimuthally varying field (AVF) cyclotron

4.1 Hill and valley

As we have seen, in the isochronous cyclotrons, we have a radial field component B_r that gives a vertical defocusing force: $F_z \propto z$. This defocusing force is linear in z (like a defocusing quadrupole). In order

to compensate the defocusing force, one can theoretically add a new vertical force $F_z^{new} = q\, v_r\, B_\theta$ with a new field component B_θ

$$F_z = q\,(\,v_\theta \cdot B_r - v_r \cdot B_\theta\,) \quad . \tag{I.13.44}$$

A modulation of the magnet yoke gap, function of the azimuth θ produces such B_θ component. If we build a magnet gap modulation adding N angular sectors, i.e. a succession of hills and valleys, the vertical field is modified and can be described as

$$B_z(R,\theta) \;=\; B_0\,[1 \;+\; f\sin{(N\theta)}] \quad . \tag{I.13.45}$$

Due to ($\nabla \times B \;=\; 0$), this produces an azimuthal field $\;, B_\theta \;=\; z\,\frac{dB_z}{R\,d\theta} \;=\; +\frac{B_0}{R}\,f\,N\,\cos(N\theta)$. The sign of this components is oscillating in the sectors.

Besides, the local orbit curvature radius $\rho(\theta)$ in the high field sectors (hill) is reduced, since locally we have $\rho_{\text{hill}} \;=\; \frac{B\,\rho}{B_z} \;=\; \frac{B\,\rho}{B_0(1+f)} \;\simeq\; R_0\,(1-f)$. While, in the low field region (valley) $\rho_{\text{valley}} \;\simeq\; R_0\,(1+f)$. The evolution of the trajectory radius corresponds to a radial velocity $v_r \;=\; \frac{dR}{dt}$, whose sign changes periodically.

Therefore the combination of the two effects generates a new vertical force $F_z \;=\; -q\,(v_r\,B_\theta)$ that is always focusing vertically (see Fig. I.13.8). This effect has been discovered by L.H. Thomas in 1938, and has improved greatly the transmission of the early cyclotrons.

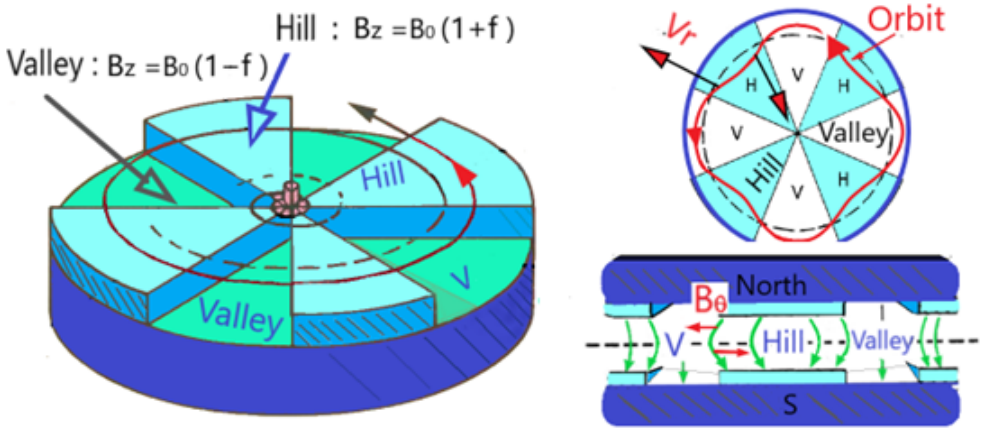

Fig. I.13.8: Principle of pole modulation with a "4 straight sectors" cyclotron. The pole modulation generates two effects: 1) An oscillation of the trajectories in the horizontal plane corresponding to the non-circular orbit $v_r \;=\; dR/dt \;\neq\; 0 \quad (v_r \;<\; 0$ at the hill entrance and $v_r \;>\; 0$ at the exit). 2) An angular field component proportional to z: $B_\theta \;=\; z\,\frac{dB_z}{R\,d\theta} \;+\;\ldots$ The so created force F_z is always opposite to z (this is a vertical focusing force): $F_z^{AVF} \;=\; q\,(-\,v_r\,B_\theta) \sim\; -\,z$.

4.2 Flutter F and averaged field index k

The effect of the vertical focusing is maximal when the particle crosses the edge of a sector, and zero in its middle. The evaluation of the average focusing effect over one turn, is related to the flutter function $F(R)$ defined as the relative mean-square azimuthal fluctuation of the magnetic field B_z along a circle

of radius R

$$F(R) \;=\; \frac{\langle (B_z(R,\theta) \;-\; \langle B_z(R,\theta)\rangle)^2\rangle}{\langle B_z(R,\theta)\rangle^2} \;=\; \frac{\sigma^2_{B_z}}{\langle B_z\rangle^2} \quad . \tag{I.13.46}$$

Here $\langle B_z(R,\theta)\rangle \;=\; \frac{1}{2\pi}\int_0^{2\pi} B_z(R,\theta)d\theta \;=\; B_0$ is the average field value over one turn.

The flutter $F(R)$ is an useful quantity: since the tune Q_z is connected to the betatron oscillation frequencies it can be expressed quite precisely in terms of $F(R)$. The local curvature radius $\rho(\theta)$ in a complex field $B_z(\theta)$ does not coincide anymore with the radius R (the coordinate R). Let us define an equivalent radius $\langle R\rangle$ connected to the path length C over one turn: $\langle R\rangle \;=\; \frac{C}{2\pi}$.

The magnetic rigidity corresponds to the product of the average field and radius

$$B\,\rho \;=\; p/q \;=\; \langle B(\theta)\rangle\,\langle R\rangle \quad . \tag{I.13.47}$$

The demonstration comes easily, since locally $B(\theta) \;=\; B\,\rho/\rho(\theta)$, we compute the average field

$$\langle B\rangle \;=\; \frac{1}{C}\int B\,ds \;=\; \frac{B\,\rho}{C}\int \frac{1}{\rho(\theta)}\,ds \;=\; \frac{B\,\rho}{C}\int_0^{2\pi}\frac{1}{\rho(\theta)}\,\rho\,d\theta \;=\; \frac{B\,\rho}{C}\,2\,\pi \;=\; \frac{B\,\rho}{\langle R\rangle} \quad . \tag{I.13.48}$$

Exercise n^o5: Flutter calculation

Considering a four-sector cyclotron with the field: $B_Z(R,\theta) \;=\; B_0\,[1 + f\,\cos(N\theta)]$, where $N = 4$. compute the "flutter" $F(R)$.

Answer:

First, we know the average field $\langle B_z(R,\theta)\rangle \;=\; B_0(R)$. Let's evaluate the value $\langle\sigma^2_{B_z}\rangle$

$$\langle (B_z - \langle B_z\rangle)^2\rangle = \frac{1}{2\pi}\int_0^{2\pi} (\,B_0[1 + f\,\cos(N\theta)] - B_0\,)^2\,d\theta$$

with $N = 4$.

We need to compute the integral of $\cos^2$, remembering $\cos(N\theta) = \frac{\exp(iN\theta)+\exp(-iN\theta)}{2}$, we get $\cos^2(N\theta) = \frac{1+\cos(2N\theta)}{2}$.

The flutter is then: $F \;=\; \frac{\langle (B_z-\langle B_z\rangle)^2\rangle}{\langle B_z\rangle^2} \;=\; \frac{1}{2\pi}\int_0^{2\pi}[f\,\cos(N\theta)]^2\,d\theta \;=\; \frac{f^2}{2}$.

Whatever the sector number N , we have always $F = f^2/2$.

We generalize this result with a more complex field, taking

$$B_z \;=\; B_0\,[1 + \sum A_n(R)\cos(n\theta) + B_n(R)\sin(n\theta)]$$

the flutter would be $F(R) \;=\; \sum_n \frac{A_n^2+B_n^2}{2}$.

Though the trajectories are complex in an AVF cyclotron, a simple formula holds: $B\rho \;=\; \langle B\rangle\langle R\rangle$. The field index should now be defined as an average and the field evolution is calculated over one turn

$$\langle B_z \rangle \, = \, \langle B_0 \rangle \, \left(\frac{\langle R \rangle}{\langle R_0 \rangle} \right)^k \quad .$$

Locally in a magnet, we still use the local field index n

$$n(\rho, \theta) \, = \, - \frac{dB}{d\rho} \, \frac{\rho}{B} \quad ,$$

where $\rho(\theta) \, = \, \frac{B\,\rho}{B_z(\theta)}$ is the local curvature radius in the magnet. While in an AVF machine the average field index k over one turn is

$$k(\langle R \rangle) \, = \, + \left(\frac{dB}{d\langle R \rangle} \right) \left(\frac{\langle R \rangle}{B} \right) \quad ,$$

where $\langle R \rangle \, = \, \frac{1}{2\pi} \int ds$ is the average radius.

Note on sign convention: Let us underline the sign + of k corresponds to the convention of the synchrotron community and is not coherent with n: $\langle B_z \rangle \propto \langle R \rangle^k$ and $B_z \propto \rho^{-n}$ (sorry...).

Exercise $n^o 6$: Average field index k in a Separate Sector Cyclotron (S.S.C.).

Compute the average field index k, in a separated sector cyclotron (sometimes called "ring cyclotron").

Answer:

In a cyclotron without azimuthal field modulation, the trajectories are circular, and we have $B_z(\theta) \, = \, \langle B \rangle$ and $\langle R \rangle \, = \, \frac{B\rho}{\langle B \rangle} \, = \, \rho$, so $k \, = \, - \, n$. In a Separated Sector Cyclotron with N radial sectors, the trajectories alternate straight lines of length L_0 and circular sections with $\Delta \, = \, 2\pi / N$. The path for a reference particle is $C \, = \, 2\pi \, \rho \, + \, N \, L_0 \, = \, 2\pi \, \langle R \rangle$. The constant factor $\lambda \, = \, \langle R \rangle / \rho$ drives the field in the sectors: for a given trajectory, we have $B_{\text{sector}} \, = \, \frac{B\rho}{\rho} \, = \, \frac{\langle B \rangle \langle R \rangle}{\rho} \, = \, \lambda \, \langle B \rangle$.
We have demonstrated in the text that $B \, \rho \, = \, \langle B \rangle \langle R \rangle$, therefore

$$\langle R \rangle \, = \, \frac{B \, \rho}{\langle B \rangle} \, = \, \frac{\gamma \, m \, v}{q \, \langle B \rangle}.$$

Using the average radius $\langle R \rangle$ the particle revolution is given by

$$\omega \, = \, 2\pi \, F_{\text{rev}} \, = \, \frac{v}{\langle R \rangle} \, = \, \frac{q \langle B \rangle}{m \, \gamma}.$$

For isochronism (ω = constant), we should have $\langle B \rangle \, = \, B_0 \gamma \, \langle R \rangle$. Finally, we obtain the same formula for k in an AVF than the field index n in an uniform field cyclotron (except for the sign convention)

$$k(\langle R \rangle) \, = \, + \left(\frac{d\langle B \rangle}{d\langle R \rangle} \right) \left(\frac{\langle R \rangle}{\langle B \rangle} \right) \, = \, \gamma^2 \, - \, 1 \qquad \text{(see Ex. } n^o 4\text{)}.$$

4.3 Edge focusing and AVF cyclotron

The mechanism of vertical focusing in a cyclotron with straight radial sectors is very similar to the edge focusing that occurs at the entrance and exit of the rectangular bending magnets in a synchrotron.

A dipole magnet, that has an entrance edge non-perpendicular to the reference trajectory, generates focusing or defocusing depending on the sign of the edge angle.

In the deviation plane (horizontal), a positive edge corresponds to less deviation of external trajectories ($x > 0$), which has the same effect as that of a defocusing lens (see Fig. I.13.9).

With a positive entrance edge angle ($\beta_1 > 0$), like a rectangular dipole magnet, the focal length associated in the horizontal plane is

$$f_x = -\frac{R_0}{\tan\beta_1} \quad .$$

Like in a quadrupole, the effect in the vertical plane is inverse to the one in horizontal plane and the edge is vertically focusing (see Chapter I.3 on transverse beam dynamics for a full demonstration).

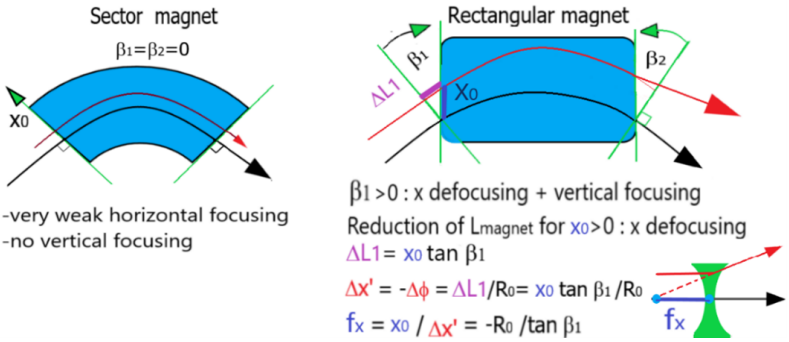

Fig. I.13.9: In a sector magnet, the edge crossing has no effect. In a rectangular dipole magnet a positive edge angle at entrance β_1 and exit β_2 defocuses in the horizontal plane ($f_x < 0$), and focuses in the vertical plane ($f_y > 0$).

Exercise n^o7: Transfer matrix R of a dipole magnet with edges

Write the transfer matrix R for a dipole magnet with a positive entrance edge angle β_1 in the vertical plane $(y, y') = \mathbf{R}(y, y')$ in a thin lens approximation.

Answer: At the edge, the vertical angle change $\Delta y'$ is given by

$$\Delta y' = -\frac{y_0}{f_y} = -\frac{y_0}{\left(\frac{R_0}{\tan\beta_1}\right)}.$$

After the dipole edge, $y = y_0$ and $y' = -y_0 \frac{\tan\beta_1}{R_0} + y'_0$.
This can be represented in matrix form

$$\begin{pmatrix} y \\ y' \end{pmatrix} = \begin{pmatrix} 1 & 0 \\ -1/f_y & 1 \end{pmatrix} \begin{pmatrix} y_0 \\ y'_0 \end{pmatrix} = \begin{pmatrix} 1 & 0 \\ -\frac{\tan\beta_1}{R_0} & 1 \end{pmatrix} \begin{pmatrix} y_0 \\ y'_0 \end{pmatrix}.$$

In the AVF cyclotrons, the crossing of an *hill edge* is such that the equivalent edge angle β is positive.We can demonstrate (see Ex. n°8) that the vertical tune is

$$Q_z^2 \;=\; -\,k \;+\; \frac{1}{2}\,f^2\,\frac{N^2}{N^2-1} \;=\; -\,k \;+\; F\,\frac{N^2}{N^2-1} \quad . \tag{I.13.49}$$

Exercise $n^o 8$: Q_z in an AVF Cyclotron

Computation of the vertical tune in an AVF field: $B_z(R,\theta) = B_0\,[1 + f\sin(N\theta)]$

- First, compute a periodic solution for the radial motion $R = r(\theta)$,
- Then, compute the particle dynamics in the vertical plane.

Answer:

The field perturbation in AVF generates $\delta F_r = -qv_\theta\,\delta B_z = -qv_\theta\,B_0 f\sin(N\theta)$. The expected evolution is $R = R_0 + x(t) = R_0 + A\sin(N\omega t)$. Let's compute A. The effect of the field index k is neglected radially because the smooth variation of $B(R)$ is smaller than the variation of $B(\theta)$ for the equilibrium orbit

$$\frac{d^2x}{dt^2} = -\omega^2 x - qv_\theta B_0\frac{f\sin(N\theta)}{m\gamma} = -\omega^2 x - \omega^2 R_0 f\sin(N\theta),$$

(since $v_\theta = R_0\,\omega$ and $\omega = \frac{qB_0}{m\gamma}$)

$$-\omega^2 N^2 A\sin(N\theta) = -\omega^2 A\sin(N\theta) - \omega^2 R_0\,f\sin(N\theta).$$

Then,

- The amplitude is: $A = \frac{fR_0}{(N^2-1)}$.
- The radial velocity is: $v_r = \frac{dR}{dt} = \frac{d\theta}{dt}\frac{dR}{d\theta} = \omega N A\cos(N\theta)$.
- The azimuthal field is: $B_\theta = z\frac{dB_z}{Rd\theta} = +\frac{z\,B_0\,Nf\cos(N\theta)}{R_0}$.
- The vertical force is: $F_z^{\text{AVF}} = -qv_r B_\theta = -\omega z q\langle B\rangle A f N^2\cos^2(N\theta)$.

Compute the vertical motion $z(t)$ as in Section 3.4

$$\frac{d^2z}{dt^2} = -\omega^2\,Q_z^2\,z = -\omega^2 z\,n\,z + \frac{F^{\text{AVF}}}{m\gamma} = -\omega^2 nz \;-\; \omega^2 z\,f^2\cos^2(N\theta)\frac{N^2}{N^2-1}.$$

The average effect over one turn is

$$\langle\frac{F^{\text{AVF}}}{m\gamma}\rangle = \langle\,\omega^2 z\,f^2\frac{N^2}{N^2-1}\cos^2(N\theta)\,\rangle = -\omega^2 z\,\frac{f^2}{2}\frac{N^2}{N^2-1} = -\omega^2 z\,F\frac{N^2}{N^2-1}.$$

Finally, we obtain: $Q_z^2 \;=\; \langle n\rangle + F\frac{N^2}{N^2-1} \;=\; -k + F\frac{N^2}{N^2-1}$.

4.4 Spiral sectors on the poles of a compact cyclotron magnet

We can use edges with a spiral shape on the pole modulations of the AVF machines to enhance the vertical focusing effect over one turn. Shifting progressively the hill boundary with a function $g(R)$ gives a field

$$B_z(R,\theta) = B_0\,[1 + f\,\sin(N(\theta - g(R)))] \quad . \tag{I.13.50}$$

Figure. I.13.10 helps in understanding the effect due to a spiral modulations of the poles (sectors):

- At each hill entrance, we have a vertical defocusing due to the field boundary not being perpendicular to the particle trajectory (the inclination angle is negative $\xi < 0$);
- At each hill exit, we have a vertical focusing ($\xi > 0$): the spiral edge of the pole enhances the vertical focusing (see exercise n°7) increasing the crossing angle β between the edge and the trajectory. The focal length F_{edge} of one edge is the sum of the two contributions AVF+ spiral edges.

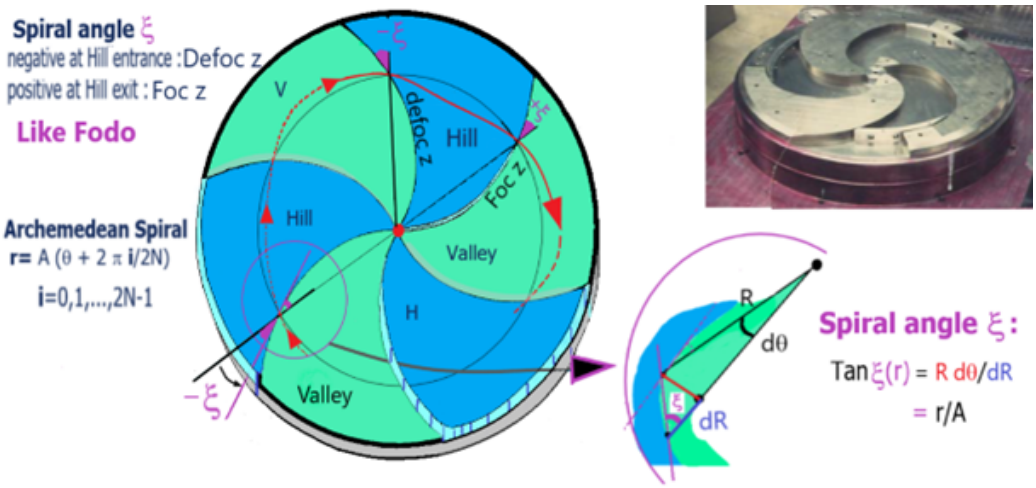

Fig. I.13.10: Effect of spiral modulations of the magnet pole ξ. The sector edges produce an alternate focusing. The spiral edge angle generates an additive radial field component $B_r = -B_\theta \tan\xi$, and forces $F_z \propto -v_\theta\, B_r$. The inclination of the sector edge ξ is related to the shape of the edge $g(R)$. For an Archimedean spiral $g(R) = R/A$, the global focusing effect increases with radius since the inclination $\tan(\xi)$ increases with the radius R. The pole of the "C01" cyclotron Ganil (France) is reproduced in the right corner.

The overall effect of spiral edge "Defocus-Focus…" is focusing. Like in a FODO channel where the effect of two lenses with alternate polarities, and separated by a distance L, is always focusing. The transport matrix element R_{21} of a FODO is negative (focusing)

$$R_{21} = \frac{-1}{F_{FODO}} = \frac{-1}{F} + \frac{1}{F} - \frac{L}{2F^2} = -\frac{L}{2F^2} < 0 \quad . \tag{I.13.51}$$

For the spiral geometry, we can use an Archimedean spiral $g(R) = \frac{R}{A}$, for which the inclination of the field boundary to the particle trajectory becomes

$$\tan\xi(R) = \frac{R\,d\theta_{\text{edge}}}{dR} = R\frac{d\,\frac{R}{A}}{dR} = \frac{R}{A} \quad .$$

In an Archimedean spiral, the tangent of the spiral angle ξ increases linearly with radius and the associated z-focusing effect increases at large radius, compensating the increase of the relativistic vertical defocusing effect.

4.5 Separated Sector Cyclotron (SSC), sometimes called ring cyclotron

When the Lorentz factor becomes large ($\gamma > 1.4$) we have to increase the flutter term F to keep an efficient vertical focusing. This is possible by reducing the field in the valley down to zero: separating the sectors leads to the Separated Sector Cyclotron (see for example Fig. I.13.11 or Fig. I.13.5). The SSCs providing optimal beam quality are apt to accelerate high-energy beams. They require generally a pre-accelerator for the beam injection. Let's consider a Separated Sector Cyclotron with the following field: $B_z = B_0\,[1 + f\,\sin(N\theta)]$ with $f \sim 1$.

The field in the hill region ($B_{\text{hill}} = B_0\,[1+f]$) is limited by the magnet technology, and the corresponding average field is rather low due to the significant amplitude variation ($f \sim 1$)

$$\langle B_z\rangle = B_0 = \frac{B_{\text{hill}}}{1+f} \quad . \tag{I.13.52}$$

Consequently a SSC provides a better focusing than a "compact" AVF that have only one magnet. But the SSC dimensions are larger (radius) for a given energy, because of a lower average field $\langle B_z\rangle$.

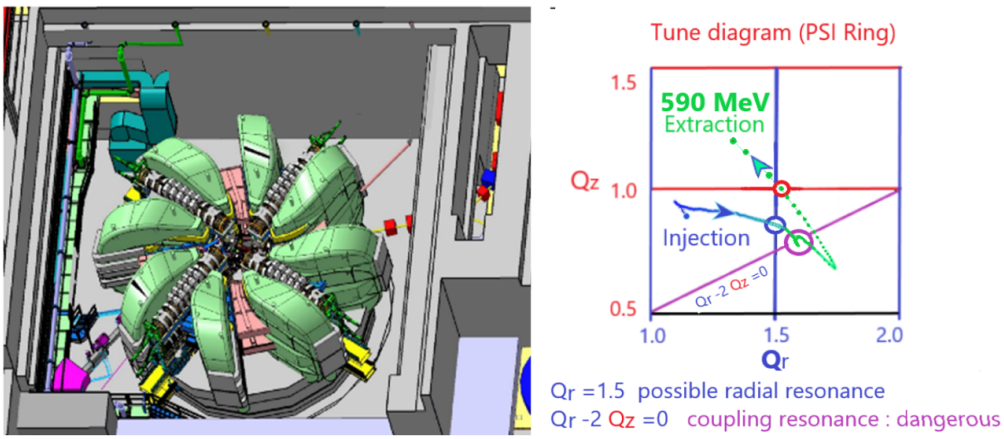

Fig. I.13.11: PSI Ring cyclotron and tune diagram. The largest cyclotron of the Paul Scherrer Institute (PSI, Villigen, Switzerland) provides a very intense proton beam (up to 2.5 mA) at 590 MeV. The total size of the accelerator is about 15 m in diameter ($R_{\text{extraction}} = 4.5$ m). It is composed by 8 independent and separated magnets with a spiral shape, to increase as much as possible the z-focusing. Besides four RF cavities in the valleys are required for a single-turn extraction to reduce the beam losses. The large beam power permit to produce high intensity secondary particles (neutrons, muons, pions) for different research fields. The right part of the figure shows that the tunes, i.e. the number of oscillations per turn in z and r, vary during acceleration; for certain radii (corresponding to values like $Q_r = 1.5$), resonances may be excited causing oscillations and beam losses (see Section 4.7).

4.6 Tunes in AVF cyclotrons with spiral sectors

After complex calculations, the vertical and radial tunes in AVF cyclotrons with N sectors are

$$Q_z^2 = -k + \frac{N^2}{N^2-1} F \left(1 + 2\tan^2(\xi) + \dots\right) \quad , \tag{I.13.53}$$

$$Q_r^2 = 1 + k + \frac{3N^2}{(N^2-1)(N^2-4)} F \left(1 + 2\tan^2(\xi) + \dots\right) \quad . \tag{I.13.54}$$

- The term $\frac{1}{N^2-4}$ in the radial tune means that a cyclotron geometry with two sectors ($N = 2$) is unstable in the horizontal plane. Therefore, $N = 3$ sectors is the minimal geometry.
- In an isochronous cyclotron, the average field index k is constrained by the isochronous requirement $k = \gamma^2 - 1$ (see exercises 4 and 6).

4.7 Tunes and resonances

The tune calculation is important to establish whether the vertical motion is stable (${Q_z}^2 > 0$), but it is not sufficient. At a certain energy and if the tunes reach an integer value ($Q = N$) it means that any particle will return nearly at the same position after one turn: So if one of the magnets has a field defect (no magnet is perfect) the particles will see the same defect at each turn, producing large amplitude oscillations and finally beam losses. Moreover, if the tune corresponds to $Q_z = \frac{N}{K}$, i.e. the particles will return to the same vertical position after K turns, this can excite a resonance. K is the resonance order.

In a machine with large turn numbers, the oscillations in the vertical plane can even excite the horizontal resonances (non-linearities couple the vertical and horizontal motions). Thus in synchrotrons and cyclotrons, we adjust the tunes to avoid a resonance, by requiring $K\,Q_r + L\,Q_z \neq N$ during the acceleration, where K,L,N are integers. In a synchrotron, the tunes are nearly constant, while in a cyclotron the tunes evolve progressively. Only a large cyclotron with a large turn number ($N_{\text{turn}} > 500$) can excite a resonance, while in a synchrotron this is more important since the particles perform more than 10^7 turns in a large number of identical cells. The low order resonances are the most dangerous ($|K| + |L| = 1, 2, 3$), since these can appear after a few turns. In the PSI ring cyclotron, see Fig. I.13.11, the most dangerous resonance corresponds to $Q_r - 2Q_z = 0$, since during the acceleration the beam remains a long time around this value, and a small beam deviation from the ideal value, can generate large amplitude oscillations due to this coupling resonance.

4.8 Limits of the tunes formulas

The previous approximations for Q^2 are not very precise, since these formulas correspond to a simplified field: $B_z(R,\theta) = B_0\,[1 + f\,\sin\left(N(\theta - g(R))\right)]$.

In reality, the magnetic field description of real magnets is often more complex than one sinusoidal function. General formulas have been computed for a field with several harmonics [7]. Besides RF cavities produce as well a weak focusing effect [8].

For a more accurate determination of the tunes $Q_{z,r}$, we can simulate numerically few trajectories. With a multiparticle code using a realistic field map, we extract the first order transport matrix $\mathbf{R}$ over one turn: we use a reference particle, which describes a closed orbit (the trajectory comes back at the same position after one turn without acceleration). The dynamics is periodic without acceleration and the matrix over one turn has the following form

$$\mathbf{R}(0,2\pi) = \begin{pmatrix} \cos(\mu) + \alpha\sin(\mu) & \beta\sin(\mu) \\ \gamma\sin(\mu) & \cos(\mu) - \alpha\sin(\mu) \end{pmatrix} \quad . \tag{I.13.55}$$

Where (α, β, γ) are the Twiss parameters. For instance, two particles starting at two different horizontal positions and sent over one orbit allow us to extract $R_{11} = \frac{(x_1 - x_0)_{\text{final}}}{(x_1 - x_0)_{\text{initial}}}$. The phase advance per turn $\mu = 2\pi Q$ is obtained by calculating half the trace of the transport matrix

$$\cos(\mu_r) = \frac{1}{2}\,\text{Trace}(\mathbf{R}) = \frac{1}{2}\,(R_{11} + R_{22}) \quad . \tag{I.13.56}$$

Finally, we can compute the tunes with the numerical evaluation of the transport matrix: thus, we can extract μ_z and μ_r

$$Q_{z,r} = \frac{\mu_{z,r}}{2\pi} = \frac{\arccos\left(\frac{1}{2}\,\text{Trace}\,\mathbf{R}\right)}{2\pi} \quad . \tag{I.13.57}$$

Another limit of the tunes formulas can be underlined: the tune concept does not describe fully the particle motion, since it is a first order approach. The complexity of the cyclotron magnet and the complexity of the trajectories with the acceleration produce many non-linear effects. Therefore, a start-to-end multi-particle simulation is always required.

5 Frequency modulated cyclotrons (not isochronous)

With some modifications to cyclotrons, two new machines solve the problem of the detuning between particle revolutions and RF-field by cycling the RF frequency: synchrocyclotron and Fixed Field Alternating Gradient (FFAG) accelerators [11–13].

5.1 Synchrocyclotron

The RF modulated cyclotrons called synchrocyclotrons[5] are nowadays less used than the isochronous cyclotrons. In the synchrocyclotron, the magnetic field is not shaped for isochronism, and the RF frequency F_{rf} varies to synchronize the few injected bunches during their acceleration

$$\omega_{\text{rev}} = \frac{q\,B_0}{m\,\gamma(R)} = f(\text{Radius}) = f(\text{time}) = \frac{2\pi F_{\text{rf}}(t)}{H} \quad . \tag{I.13.58}$$

During one cycle, the RF frequency is first adapted to the injection energy ($\gamma = 1$). Progressively, the

[5]Historical note: The synchrocyclotrons were the precursors of the synchrotrons, they provided the highest energy particle beams from 1946 to 1954. The first accelerator of the CERN facility was a 600 MeV proton synchrocyclotron with a radius of 2.3 m and had been operational in the years 1957–1990. Nowadays, for research applications, which require often a high beam intensity, the 100% duty cycle isochronous cyclotron are preferred. Regarding very high-energy applications, synchrotrons have still no rival.

frequency is decreased to follow the evolution of the γ factor of a given particle. The frequency then reaches the value corresponding to the extraction energy. Then, the frequency restarts to its highest value to be re-synchronized for the acceleration of the next few other bunches.

Any particle injected at RF phase φ close to an ideal phase φ_s will oscillate during the acceleration. This is the synchrotron oscillations. The phase φ_s is called "synchronous phase" and corresponds to a particle phase such as to allow to cross the gaps at the same RF phase during the whole acceleration process. The particle revolution period $T_{\rm rev}$ is not constant during the acceleration.

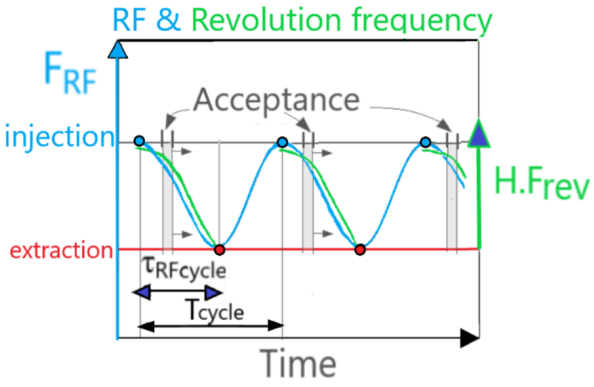

Fig. I.13.12: The cycle of the RF frequency in a synchrocyclotron. Few bunches are injected when the RF frequency is at its maximun, then the frequency is decreased to follow the particle revolution frequency.

The revolution frequency of a given particle in a synchrocyclotron decreases with $\gamma(R)$ from the injection to extraction radius. For a good acceleration the RF frequency should decrease, as well, to match the behaviour of the revolution frequency. For a given particle the total acceleration ΔE should take place during the decreasing part of the RF cycle $\tau_{\rm RFcycle}$. The energy gain per turn must be on average

$$\langle \delta E_{\rm turn} \rangle \;=\; \frac{\Delta E}{N_{\rm turn}} \;\text{with}\; N_{\rm turn} \;=\; \frac{\tau_{\rm RFcycle}}{\langle T_{\rm rev} \rangle} \quad . \tag{I.13.59}$$

The energy gain per turn is related to the gap number $N_{\rm gap}$, the cavity aperture $\alpha_{\rm cav}$, and the RF voltage

$$\langle \delta E_{\rm turn} \rangle \;=\; q\, N_{\rm gap}\, U_0\, \sin\left(\frac{H\,\alpha_{\rm cav}}{2}\right) \cos(\langle \phi \rangle) \;=\; q\, V_0\, \cos(\varphi_s) \quad . \tag{I.13.60}$$

Technically, the cycle of RF can hardly be faster than 1 kHz and the acceleration must take a rather long time $\tau_{\rm RFcycle} \sim$ 1 ms in order to synchronize the particle revolution frequency with the RF (see I.13.12). In comparison, the revolution period is short $\langle T_{\rm rev} \rangle = \frac{H}{\langle F_{\rm rf} \rangle} \sim$ 10-20 ns, finally the beam performs a large number of turns in the synchrocyclotron

$$N_{\rm turn} \;=\; \frac{\tau_{\rm RFcycle}}{\langle T_{\rm rev} \rangle} \;\sim\; 10^4 \;-\; 10^5 \quad . \tag{I.13.61}$$

The total acceleration voltage V_0 per turn and the synchronous phase ϕ_s are chosen to match the cycle of the RF (I.13.12), therefore the energy gain $\delta E_{\rm turn}$ must be small

$$\langle \delta E_{\text{turn}} \rangle = qV_0 \cos(\varphi_s) = \frac{\Delta E}{N_{\text{turn}}} = (E_{\text{extraction}} - E_{\text{injection}}) \frac{\langle T_{\text{rev}} \rangle}{\tau_{\text{RF cycle}}} \quad . \tag{I.13.62}$$

The couple (V_0, φ_s) have to fullfil the equation: $q\,V_0\,\cos(\varphi_s) = \Delta E \frac{T_{\text{rev}}}{\tau_{\text{RFcycle}}}$. The synchronous phase φ_s should be chosen to maximise the phase acceptance of the synchrocyclotron: the typical value of $\varphi_s = 60\,^{\circ}$provides a large acceptance in phase such that many particles having different phases at the source output will be captured and will describe stable oscillations in the plane (phase, energy) [2]. The frequency Ω_{synchro} of the synchrotron oscillations is generally much lower than the revolution frequency: $\Omega_{\text{synchro}} \sim 10^{-3}\,\omega_{\text{rev}}$.

The main drawback of a synchrocyclotron is its low duty cycle. Because of the frequency variation of the cavity, only a small fraction of the charged particles leaving the source are synchronized with the RF acceleration. As an advantage, the magnet of a synchrocyclotron can be much simpler than the one for isochronous ones.

For the proton therapy facilities, the IBA company proposes an ultra-compact superconducting synchrocyclotron called "S2C2" [16] and can be operated at 5 Teslas (see Fig. I.13.13).This new machine aims to replace the less compact isochronous superconducting cyclotron “C235” (see Fig. I.13.14).

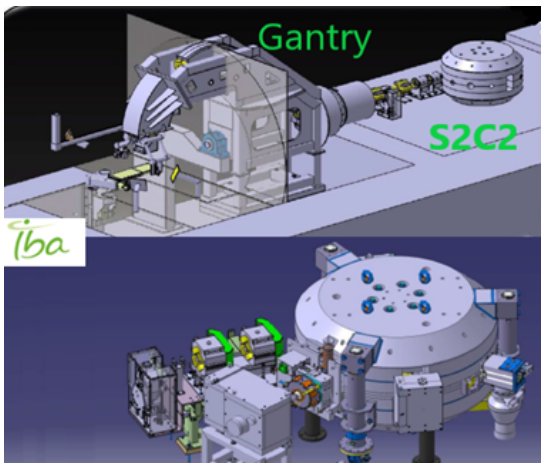

Fig. I.13.13: The S2C2® IBA proton synchrocyclotron and the associated rotating gantry. This machine, because of the very high field, is more compact than an isochronous cyclotron, but it has a very low duty cycle. Accelerator parameters: $E_p = 230\,\text{MeV}$; the total weight is 50 tons. The field at extraction $\langle B \rangle = 5\,\text{T}$, average field index $k < 0$. Extraction radius $R = 49\,\text{cm}$. The RF frequency is cycled $F_{\text{rf}} = [93\,\text{MHz}, 63\,\text{MHz}]$. The repetition rate is $1\,\text{kHz}$. Duty cycle $= 0.7\%$. The beam pulse duration is $T_{\text{pulse}} = 7\,\mu\text{s}$. The Dee voltage is very low $V_{\text{rf}} = 10\,\text{kV} \rightarrow$ number of turns ~ 40000.

Fig. I.13.14: The C235 ® IBA isochronous cyclotron. This proton cyclotron has 100 % duty cycle but has a greater cost than the very compact synchrocyclotron "S2C2". Accelerator parameters: $E_p = 235$ MeV; the total weight is 210 tons.The average field at extraction is $\langle B \rangle = 2.2\,\mathrm{T}$, average field index $k > 0$. A compact magnet with spiralled sectors is used. Extraction radius $R = 108$ cm (duty cycle = 100%). The RF frequency is fixed $F_{\mathrm{rf}} = 106\mathrm{MHz}$, and the Dee voltage is $V_{\mathrm{rf}} = 150\,\mathrm{kV}$. The beam performs about 700 turns to reach the extraction channel.

6 FFAG: Fixed Field Alternating Gradient accelerator

The idea of FFAG [11–13] (also abbreviated FFA) is to provide a very high energy like in a synchrotron ($\gamma \gg 1$) but at a higher duty cycle. The ramping of the magnets of a synchrotron limits the repetition rate to a range 1Hz - 50Hz. Instead in a FFAG or a synchrocyclotron the magnet field is constant in time, and the cycling of the RF can be as fast as 1 kHz. The vertical focusing in synchrocyclotron is not optimal, and an FFAG provides a better beam quality at even larger energy. The FFAG idea has been proposed in the 1950s [14]. Few proofs of principle machines have so far been built (KURRI at KEK(Japan) with 30 and 150 MeV protons, EMMA in Daresbury(for 20 MeV electrons). A FFAG is a synchrocyclotron with complex magnets ensuring a better focusing by an alternating gradient ($\frac{dB_z}{dR}$) of complex dipole magnets. The FFAG field should oscillates azimuthally

$$B_z(R,\theta) = \pm B_0 \left(\frac{R}{R_0}\right)^{-n} F(\theta - g(R)) \tag{I.13.63}$$

- $F(\theta - g(R))$ is a periodic oscillating function with N-fold symmetry;
- $g(R)$ is the spiral that defines the edge angles, if needed;
- $n(R,\theta)$ is the local field index in each magnet.

The average field scales as follows: $\langle B_z(\theta) \rangle = \langle B_0 \rangle \left(\frac{\langle R \rangle}{\langle R_0 \rangle}\right)^k$. The beam dynamics in a FFAG is not isochronous ($k \neq \gamma^2 - 1$).

Since we have demonstrated that $B\rho = \langle B(\theta) \rangle \langle R \rangle$, the particle momentum increases with the average radius $\langle R \rangle = \frac{C}{2\pi}$

$$P_{\mathrm{extraction}} = q\langle B_z \rangle \langle R \rangle = P_{\mathrm{injection}} \left(\frac{\langle R_{\mathrm{extraction}} \rangle}{\langle R_{\mathrm{injection}} \rangle}\right)^{k+1} . \tag{I.13.64}$$

The average field index k in a FFAG is generally rather large ($k \gg 1$) to reduce the horizontal size (and cost): for a given extraction momentum $P_{\text{extraction}}$ you can reduce $\langle R_{\text{extraction}} \rangle$ if k is large.

The vertical motion ($Q_z^2 = -k + \dots$) is stabilized with the alternating gradient magnets. The use of a series of dipole magnets (with a gradient) with alternate field $\pm B_0$ allows to provide an additive transverse focusing coming from an alternating-gradient focusing effect to obtain a stable motion ($Q_z^2 > 0$).

6.1 Scaling FFAG

The simplest idea is to find a geometry that warrants constant tunes during the acceleration (avoiding crossing resonances in the tune diagram). Scaling FFAG means that the orbit shape (optics) is kept fixed, independent of energy, just as in a synchrotron. The three conditions to obtain a constant tune are the following:

- 1) The average field index k is independent of r: by having the local index n = constant in the two dipoles $B_1 = -B_2$;
- 2) The flutter F, is independent of the radius;
- 3) A magnet with a pole shape to have a constant $\tan(\xi)$. There are two possibilities:
  - With a straight sector $\tan(\xi)$ i.e. no spiral poles for the main magnet,
  - With $r_{spiral} = R_0\, e^{A\theta}$, we get $\tan(\xi(r)) = r\,\frac{d\theta}{dr} = A$ for the reverse field magnet.

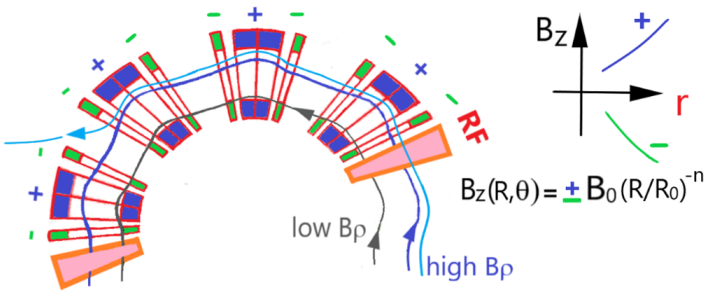

Fig. I.13.15: The scaling FFAG geometry. Unlike the cyclotrons to obtain a scaling we affect their constant focusing properties during the acceleration. An FFAG uses many cells containing a triplet of bending magnets. Positive horizontal focusing (+) in the main dipole $\frac{dB}{dR} = +n\,B_0 \left(\frac{R}{R_0}\right)^{-n} > 0$. While in the 2 reverse field dipoles (-), $\frac{dB}{dR} = -n\,B_0 \left(\frac{R}{R_0}\right)^{-n} < 0$.

The momentum compaction factor $\alpha_p = \frac{p}{C}\,(dC/dp)$, which describes the evolution of the path length C in the accelerator, scales as $\alpha_p = \frac{1}{k+1}$. This means that the path length increases monotonically with particle momentum since the average field index is fixed in scaling FFAG

$$C(p) \sim p^{\alpha_p} \sim p^{1/(k+1)} \quad . \tag{I.13.65}$$

6.2 New applications and non-scaling FFAG

In FFAG, the reverse field regions increase the average radius of the machine (and the cost) by an important factor compared to an equivalent synchrocyclotron or cyclotron. But the FFAG can be a solution when a rapid cycling synchrotron is not possible and when a cyclotron cannot reach the desired energy. For instance, FFAG accelerators were reconsidered for muons acceleration [15] for a neutrino factories and for Muon Colliders: It was indeed required to accelerate muons to an energy of about 20 GeV, not reachable with cyclotrons. The muons have a short half-life and the acceleration could be faster in a FFAG than in rapid cycling synchrotron.

The rapid acceleration with a small number of turns (< 20 turns) could be important for unstable muons ($T - 1/2 = 2.2\,\mu s$). A small number of turns allows relaxing the constraints of scaling FFAG, since the betatron oscillations and resonances will not have time to develop and spoil beam quality. Therefore, the field index can evolve $k = k(r)$. In non-scaling FFAGs, a linear variation of magnetic field can be employed: using constant-gradient "linear" magnets greatly increases dynamic aperture and simplifies construction, while employing the strongest possible gradients minimizes the real aperture. Besides, the linear field variation provides a large dynamic aperture, allowing the acceleration of large emittance beams.

The Electron Model for Many Applications (EMMA), the first non-scaling FFAG, has been built at the Daresbury Laboratory (UK) in 2010 [13]. This has become a proof of principle machine delivering $20\,\mathrm{MeV}$ electrons, and it requires a ring of 16 m circumference: The ring is composed by combined function magnets with dipole and quadrupole components (a gradient): these magnets are in fact quadrupoles, and their dipole component is obtained by using them off-axis. 42 cells composed of 2 magnets (focusing and defocusing) produce at the same time a deviation (dipolar component) and AG focusing (quadrupolar components).

The EMMA ring accelerates electrons from $10\,\mathrm{MeV}$ to $20\,\mathrm{MeV}$. EMMA has demonstrated a good stability, its geometry is called "non-scaling" since the tunes (Q_r, Q_z) vary continuously from injection to extraction. Resonance crossing happens very rapidly ($3\,Q_r = 1,\ 2\,Q_r + 2\,Q_z = 1$) within 20 turns. There are 42 cells of two magnets (quadrupoles) used off axis to provide two field components: we have $B_z(r) = B_0 \pm G\,(r - r_0)$. The alternate linear gradients $\pm\,G$ generate a small momentum compaction factor $\alpha_p = \frac{(dC/C)}{(dp/p)}$ which provides a good dynamic aperture with small magnets. Four cells of the doublet are shown in detail (https://www.technologysi.stfc.ac.uk/Pages/EMMA.aspx).

In the EMMA ring the path length decreases then increases with momentum since the average field index is not fixed like in scaling FFAG.

The path length has, in fact, a parabolic evolution $C(p) \sim Cte + \lambda(p - p_0)^2$. The parabolic evolution of $C(p)$, with a minimum, makes that the revolution frequency does not evolve monotonically. The amplitude of the evolution of the revolution is very small during the acceleration, therefore a fixed RF frequency can be used in the EMMA ring.

7 Introduction to cyclotron injection

Designing the central region of a cyclotron is a very complex task [17–22], and we present here a first approach to the injection problematic.

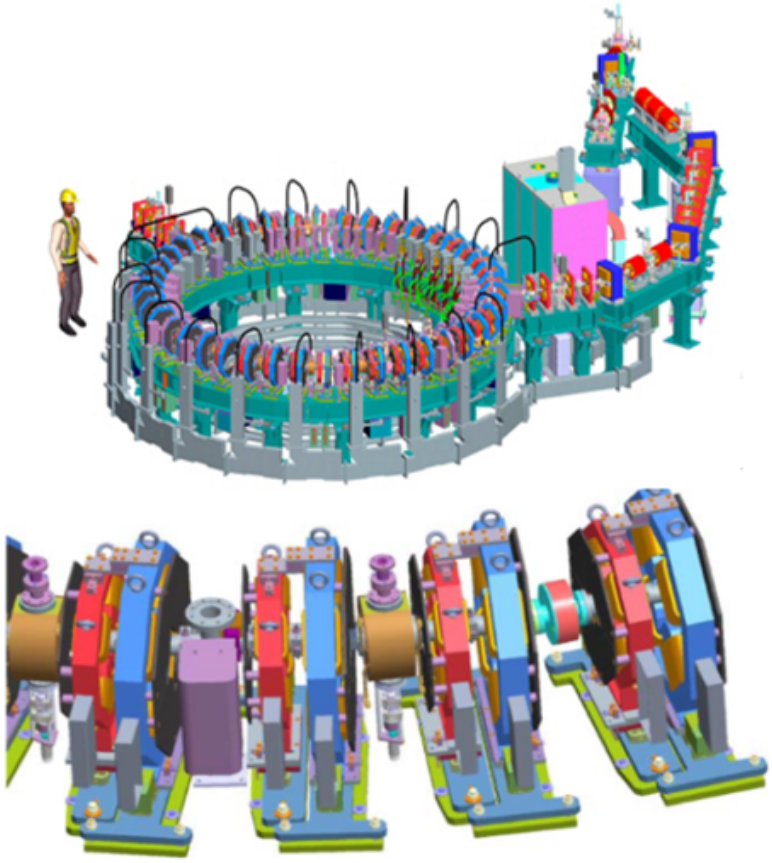

Fig. I.13.16: The EMMA FFAG constructed at STFC Daresbury Laboratory. There are 42 cells of two magnets (quadrupoles) used off axis to provide two field components: we have $B_z(r) = B_0 \pm G\,(r - r_0)$. Four consecutive doublet cells are shown in detail.

Several injection systems are used, depending of the cyclotron model.

- For the low-energy cyclotrons, two techniques are used to inject a beam in a cyclotron:
  - A very compact internal ion source inserted directly inside the cyclotron centre;
  - An external ion source connected to a beam line injects the beam axially (vertically) and bends the beam with a compact electrostatic inflector (hyperboloid or spiral inflector) on the first orbit.

- The high-energy cyclotrons (like separated sector cyclotrons) are located downstream a preaccelerator. In that case, the beam is more rigid and a compact axial injection system is not feasible. We use a radial injection beam line.

7.1 Internal ion sources

Most of industrial cyclotrons ($K_b = 5 - 30\,\mathrm{MeV}$) use a very compact internal source (PIG = Penning ion gauge, see Fig.I.13.17), which can be inserted in the central region of the cyclotron. This system

in this case does not need an injection beam line (vacuum chambers, quads, solenoids, inflector), with a large cost reduction of the accelerator. This technology can deliver positive and negative hydrogen ions.

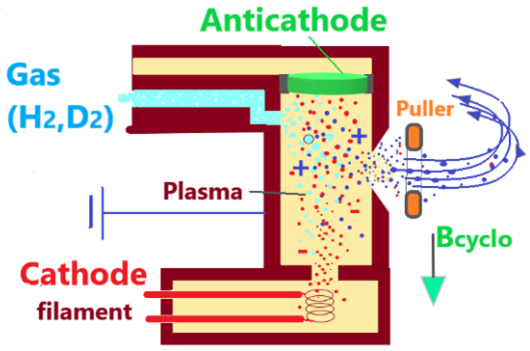

Fig. I.13.17: Penning Ion Gauge source with a hot cathode (filament). Electrons are emitted by thermoionic effect, and ionize the gas atom generating a plasma. The plasma is confined by the cyclotron magnetic field. With the electric field between the anodes and the puller ions then emerge from the plasma. This is a very old technology, but recent and specific designs are developed to improve the current or to increase the cathode lifetime, thus reducing the cost and maintenance of medical cyclotrons. A current around $I = 100$ µA is a typical performance for an H^+ beam.

7.2 Axial injection with external sources

An external ion source is often preferred for various reasons:

- An external source is less constrained geometrically and can be much larger and performing than a very compact internal ion source;
- For heavy ions it is important to obtain the highest charge state Q to increase the maximal energy of a given cyclotron: $(\frac{E}{A})_{\max} = K_b\,(\frac{Q}{A})^2$. The ECR ion source, which produces heavy ion beams with high charge states, requires a magnetic confinement with two large solenoids and a hexapolar magnet which obviously cannot fit inside a cyclotron;
- For negative hydrogen isotopes, external Multi-cusp sources are very efficient but cumbersome;
- In general, a complex injection beam line associated with an external ion source allows 6D matching (radial, axial, and longitudinal) which is better to obtain an optimal transmission. In particular, using a pre-buncher, operating at the cyclotron frequency, also permit to focus longitudinally the beam and increase the beam current and the cyclotron phase acceptance.

At the energy provided by the ion source extraction (typically 20 kV), the beam magnetic rigidity is very low. The only possibility is to inject the beam vertically toward the centre of the cyclotron, by way of a hole in the magnet yoke: in the axial direction the beam velocity is parallel to the cyclotron field B_z and no radial force perturbs the injection axially. The beam is then bent onto the cyclotron median plane with an electrostatic device, called inflector. As soon as the beam is deflected into the horizontal plane, the beam experiences a magnetic force F_r from the cyclotron field. The full motion is in 3D. After the inflector, the beam starts a circular radial motion, and meets rather quickly the first acceleration gap. The inflector is designed to inject the beam on the first cyclotron orbit R_m.

Nowadays two inflector geometries are used:

- Hyperboloid inflector (Müller inflector) [20],
- Spiral inflector (Pabot-Belmont inflector) [21, 22].

The injection geometry in a cyclotron is determined by the injection energy (the voltage of the ion source) and the mass over charge ratio of the desired beam particle: the two parameters define the magnetic rigidity at injection and the magnetic radius of the first orbit is hence $R_m = \frac{B\rho_0}{B_0}$. The inflector given the electric force generated by the inflector electrodes and magnetic force generated in the horizontal plane takes the beam to the first orbit capture.

Generally it is advisable to treat the problem of the axial injection in the backward direction:

i. Start from a trajectory rotating at large radius around cyclotron centre Ω;

ii. Then, with a simulation, propagate backward the reference particle toward the first orbit (turn): this identify the beam position just upstream of the first acceleration;

iii. Lastly, design the inflector geometry, which will take the beam from the injection beam line to the right position and angle for the first acceleration gap.

7.3 Hyperboloid inflector (called "Müller inflector")

The principle of an hyperboloid inflector [20]. is to find a geometry whose electrodes are surfaces of revolution. An hyperbolic electric potential

$$V = \frac{K_z^2}{2} + \frac{K_r^2}{4} \quad ,$$

is the simplest potential which satisfies $\Delta V = 0$ and has a radial symmetry. The two electrodes follow an equation $r^2 - 2\,z^2 =$ constant.

The central particle will stay on the equipotential surface, if the inflector satisfies two conditions:

- The initial reference velocity must be related to the inflector potential

$$v_0 = k\,\frac{r_0}{2} = \left(\frac{qK}{m}\right)\frac{r_0}{2} \quad ;$$

- The central magnetic field should match the potential

$$B_{0z} = \left(\frac{m}{q}\right) k\sqrt{6} = K\sqrt{6} \quad .$$

Assuming a constant field B_0, the motion in cylindrical coordinates of the central trajectory is described by

$$r_c(kt) = r_0\sqrt{1 + \frac{\sin^2(kt)}{2}}\;\theta_c(kt) = \frac{\sqrt{6}}{2}\,k\,t - \tan^{-1}\left(\frac{\sqrt{6}}{2}\,\tan(kt)\right)\;Z_c(kt) = \frac{1}{2}\,r_0\,\sin(kt) \quad . \tag{I.13.66}$$

In Cartesian coordinates, the central trajectory can be written as

$$\begin{cases} X_c(t) &= [a\cos(bkt) - b\cos(akt)]\,\frac{r_0}{2} \\ Y_c(t) &= [a\sin(bkt) - b\sin(akt)]\,\frac{r_0}{2} \\ Z_c(t) &= [\sin(kt)]\frac{r_0}{2} \end{cases} , \tag{I.13.67}$$

where (kt) varies in the range $[0, \pi/2]$.

The parameter k is related to the potential $V(K)$: $k = q\,K/m$. The particle trajectory is on the equipotential surface $r^2 - 2\,z^2 = r_0^2$. The parameters a, b are

$$a = (3/2)^{1/2} + 1 \quad \text{and} \quad b = (3/2)^{1/2} - 1 \quad . \tag{I.13.68}$$

The inflector height A is connected to the parameter $r_0 = 2A$. Besides A is related also to the magnetic radius R_m corresponding to the curvature radius of the first orbit: R_m is defined by the injection energy and the field of the cyclotron

$$R_m = \frac{mv_0}{qB_{0z}} = \frac{r_0}{2\sqrt{6}} = A\sqrt{6} \quad . \tag{I.13.69}$$

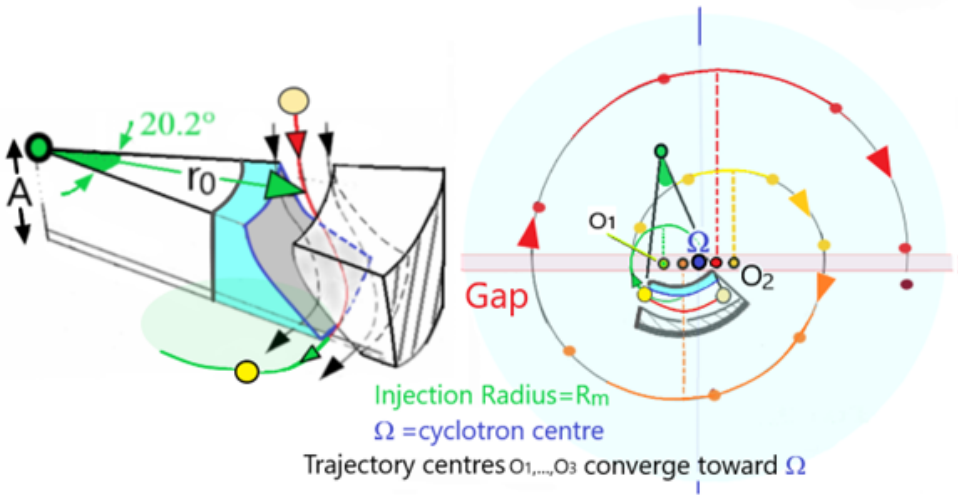

Fig. I.13.18: Hyperboloid inflector and beam centering. Left side: The inflector electrodes are represented in 3D with 3 trajectories. Right: The figure shows the geometry of the injection in a 180° Dee. The positions of the rotation centres of the ion spiral trajectory (curvature centre O_1, ..., O_3) as they move after each acceleration. The centres of curvature converge toward the cyclotron centre Ω after few accelerations.

Therefore, if R_m is fixed by the cyclotron field and the particle of interest, there is no free parameter for the geometry of the hyperboloid inflector. Generally the inflector entrance is not corresponding to the axis of the cyclotron centre Ω (off-axis injection). The position of cyclotron injection (corresponding to the inflector exit) is defined in such way that first the trajectory after several accelerations converge toward the centre of the cyclotron frame (blue circle in Fig. I.13.18). The advantage of a hyperboloid

inflector is that the two transverse sub-spaces are not correlated and can be matched independently, and the transfer matrix becomes simple (no coupling term in horizontal and vertical plane [20]. The voltage on the electrodes depends on the choice of their inter-distance $d = |r_2 - r_1|$

$$U_{\text{inflector}} = U_2 - U_1 = \left[\frac{K}{4}\right] \left(r_2^2 - r_1^2\right) \approx \left[\frac{m\,k^2}{4\,q}\right] 2r_0\,d = \left[\frac{m\,v_0^2}{q\,r_0^2}\right] 2\,r_0\,d = \frac{4\,U_{\text{source}}}{A}\,d \quad . \tag{I.13.70}$$

The hyperboloid inflector height A is sometimes too large to be adapted in a small cyclotron. In that case the more compact "spiral inflector" is preferred.

7.4 Spiral inflector (called "Pabot-Belmont" inflector)

In the spiral inflector [21, 22], the electrode shape must be such that the electric field vector $\mathbf{E}$ on the central trajectory is always perpendicular to the ion velocity vector. With this requirement the central trajectory will always lie on an equipotential surface, and this allows us to construct an inflector that works at low voltage. Several geometries can be found ensuring $\mathbf{v} \cdot \mathbf{E} = 0$. The electrodes must be tilted progressively around the central trajectory: varying the tilt adapts the geometry of the electrodes to the cyclotron constraints.

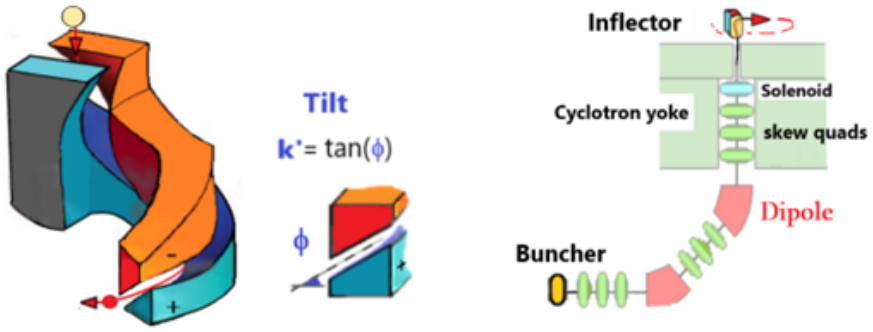

Fig. I.13.19: Spiral inflector and the electrode tilt k' . The inflector 3D geometry is shown. The frame on the right side shows a typical axial injection layout with 2 magnetic dipoles, few quadrupoles and a solenoid. For a better transmission, a RF buncher is needed upstream the cyclotron.

The electric field changes as a function of the parameter $\theta = \frac{v_0\,t}{A}$ when it varies from 0 to $\pi/2$

$$\begin{cases} E_x &= E_0\,[\cos(\theta)\,\cos(2K\theta) - k'\,\sin(\theta)\,\sin(2K\theta)] \\ E_y &= E_0\,[\cos(\theta)\,\sin(2K\theta) - k'\,\sin(\theta)\,\cos(2K\theta)] \\ E_z &= E_0\,[\sin(\theta)] \end{cases} \quad . \tag{I.13.71}$$

We can derive the parametric equation of the central trajectory in 3D. The integration of the equation of motion for the reference trajectory with $E_0 = \frac{m\,v_0^2}{q\,A}$

$$\begin{cases} X_c(t) &= -\lambda + \left[\frac{\cos(a\theta)}{a} - \frac{\cos(b\theta)}{b}\right]\frac{A}{2} \\ Y_c(t) &= \left[\frac{\sin(a\theta)}{a} - \frac{\sin(b\theta)}{b}\right]\frac{A}{2} \\ Z_c(t) &= A - A\sin(\theta) \end{cases} \quad . \tag{I.13.72}$$

The parameters (a, b, λ) are connected

$$a = 2K - 1 \quad , b = 2K + 1 \quad , \lambda = \frac{A}{4K^2 - 1} \quad . \tag{I.13.73}$$

The exit point E of the inflector in this frame is

$$\begin{cases} X_E = 2K\lambda\sin(K\pi) - \lambda \\ Y_E = -2K\lambda\cos(K\pi) \\ Z_E = 0 \end{cases} \quad . \tag{I.13.74}$$

The parameter K is related to the curvature R of the trajectory in the horizontal plane at the exit of the inflector (at $\theta = \frac{\pi}{2}$). The curvature of the trajectory R is given by two contributions: the contribution of the cyclotron magnetic field B_0 and the one of electric field E_0 of the inflector

$$K = \frac{A}{2R} = \frac{A}{\frac{2m\,v_0}{qB_0}} + \frac{A\,k'}{\frac{2m\,v_0^2}{qE_0}} = \frac{A}{2R_m} + \frac{k'}{2} \quad . \tag{I.13.75}$$

Physically, A is the inflector height, and $R_m = (m\,v_0)/(q\,B_0)$ is the magnetic radius. The tilt parameter k' is linked to the inclination of the electrodes. The electrode angle $\phi(\theta)$ in the horizontal plane changes progressively in the inflector

$$\frac{\tan\phi(\theta)}{\sin(\theta)} = k' \quad . \tag{I.13.76}$$

The tilt parameter k' is defined as the tangent of electrode angle at the inflector exit (see Fig. I.13.19)

$$k' = \tan(\phi_{\text{exit}}) \quad .$$

The parameter k' is a free parameter to adapt the entrance point of the inflector for a fixed arrival point in the cyclotron median plane. The voltage of the electrodes is computed as follows

$$U_{\text{inflector}} = U_2 - U_1 = d_0\,E_0 = d_0\,\frac{m\,v_0^2}{q\,A} = d_0\,\frac{2\,U_{\text{source}}}{A} \quad . \tag{I.13.77}$$

The parameters of the inflector are determined as follows:

- The three values ($v_0 = f(U_{\text{source}})$, $\frac{m}{q}$, B_0) define the injection radius $R_m = \frac{m\,v_0}{q\,B_0}$;
- The available space in the cyclotron hall limits the maximum height A (but decreasing A increases the required electric field and the effect of electrostatic fringe field);
- The choice of K (and k') should be determined knowing the ideal position for the centre of cur-

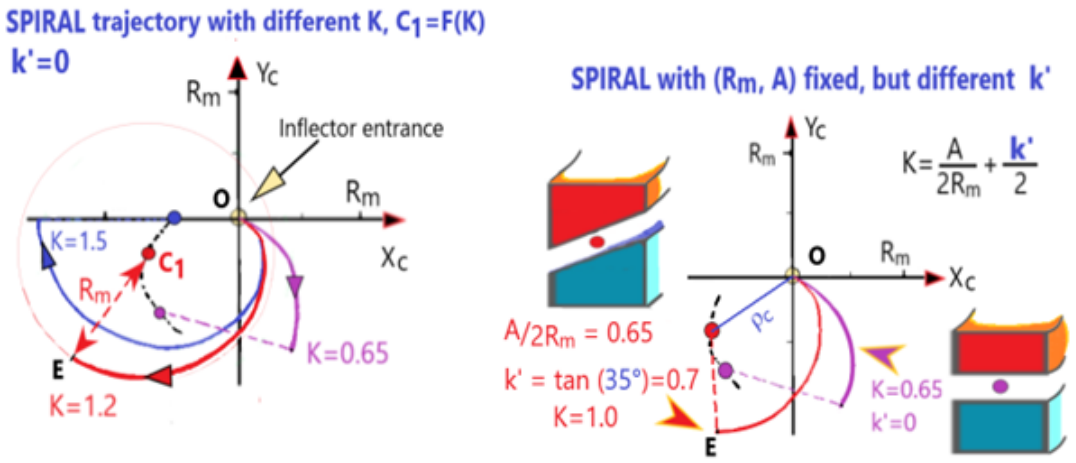

Fig. I.13.20: Spiral inflector and the electrode tilt k' . Left side: The projection of the central trajectory in the horizontal plane depends only on the two parameters (K, R_m) . The trajectory centre C_1 is depicted for 3 different K. Right side: For a given magnetic radius R_m and a given height A, the electrode tilt k' allows to reduce the distance between the inflector entrance and the trajectory centre C_1 (called off-centering ρ_c). Generally C_1 has to be close to the cyclotron centre Ω for a given inflector exit. The increase of k' reduces the off-centering ρ_c, which is a function of the 2 parameters (K, k'). The exit angle in this frame (O, x, y) is $\alpha = -K\,\pi$.

vature of the first trajectory C_1 before the first accelerating gap (the first ion curvature radius correspond R_m). The centres of curvature O_1, O_2, $O_3, \ldots$ should converge toward the cyclotron centre Ω after few accelerations (O_1 should be determined from the cyclotron simulation taking account the acceleration, and Ω does not necessarily coincide exactly to O_1).

The centre of curvature of the first trajectory C_1 (located at a distance R_m from the inflector exit) in the inflector frame is [22]

$$\begin{cases} x_{C_1} &= \left[\frac{(A - 2\,K\,A\sin(K\pi)}{1-4\,K^2} - \frac{A\,\sin(K\pi)}{2\,K-k'}\right] \\ y_{C_1} &= \left[-\frac{(2\,K\,A\cos(K\pi)}{1-4\,K^2} - \frac{A\,\cos(K\pi)}{2\,K-k'}\right] \end{cases} . \tag{I.13.78}$$

The off-centering $\rho_c = \sqrt{x_{C_1}^2 + y_{C_1}^2}$, i.e. the horizontal distance between C_1 and the inflector entrance, can be generally reduced by a rough optimization of the value of K ($K \sim 1 - 1.5$ is typical). With this choice one may place the inflector not too far from the cyclotron centre Ω.

The exit point of the inflector is fixed by the geometric constraint coming from the RF gaps. The fine tuning of k' allows to adjust the entrance position. Several solutions are found: the inflector exit should arrive tangentially anywhere on the circle (O_1, R_m).

For the centering of the inflector, a change of frame a reference is convenient, such that the inflector exit point (E) is located at the fixed position ($x' = 0$, $y' = R_m$) with a fixed direction at $0°$ whatever the parameters (A, R_m, k'). The transformation of an arbitrary point (X, Y, Z) toward the new frame (X', Y', Z') is

$$\begin{cases} X' &= (X - X_E)\cos(K\pi) - (Y - Y_E + R_m)\sin(K\pi) \\ Y' &= (X - X_E)\sin(K\pi) - (Y - Y_E + R_m)\cos(K\pi) \\ Z'_c &= Z \quad . \end{cases} \tag{I.13.79}$$

The new frame centre O' corresponds to the C_1 point. The inflector entrance O, C_1, and Ω (the cyclotron centre), have to be computed in this frame.

Though the spiral inflector is the most compact inflector, it suffers from several defects:

- The beam is often defocused vertically and requires sometimes a small electrostatic quad at the inflector exit. This requirement increases the complexity of the injection;
- The inflector transfer matrix is not analytic. Moreover, the horizontal and vertical plane being coupled, skew quadrupoles are needed in the injection beam line for a perfect transverse matching of the beam;
- The electrode geometry requires a complex machining;
- The fringe effects have to be considered, especially for short inflectors ($A < 4\,\mathrm{cm}$).

Note: The hyperboloid inflector is equivalent to a Spiral inflector having $K = \sqrt{\frac{3}{8}} = -\frac{k'}{2}$. Let us also note that the choice of the tilt parameter k' strongly affects the inflector focusing properties.

Exercise n^o9: Approximate orbit calculation in a compact cyclotron.

Compute the orbit geometry (values of trajectory radii) in a compact cyclotron having a uniform magnetic field at the injection. The cyclotron has a $180\,^\circ$ RF Dee, a turn number $N_{\text{turn}} = 25$, $R_{\text{injection}} = R_m = 3\,\text{cm}$, $R_{\text{extraction}} = 50\,\text{cm}$ and a RF-gap of $g = 2\,\text{cm}$. Compute first the energy gain after each gap. Then, discuss the influence of the transit time factor in the gap. Finally, explain how to optimize the location of the inflector exit.

Answer:

The acceleration in the first gap, that defines finally the position of the first curvature centre C_1, can be computed in a non-relativistic approximation. Let us assume a constant energy gain in the gaps during the acceleration. The average energy gain per gap is

$$\Delta E_{\text{gap}} \approx \frac{m\, v^2_{\text{extraction}}}{2}\,\frac{1}{N_{\text{turn}}\, N_{\text{gap}}} = \frac{m\, R^2_{\text{extraction}}\,\omega^2}{2\, N_{\text{turn}}\, N_{\text{gap}}}.$$

Noting that the initial radius of injection $R_0 = R_m$, the energy after the acceleration gap $n°1$

$$E_{k1} = E_{\text{injection}} + \Delta E_{gap1} = \frac{m\, R^2_m\,\omega^2}{2} + T_1\,\frac{m\, R^2_{\text{extraction}}\,\omega^2}{2\, N_{\text{turn}}\, N_{\text{gap}}}.$$

T_1 is the transit time factor in the first gap, which describes the effective reduction of the energy gain due to the variation of the electric field during the gap crossing. The transit time factors T_N are close to 1 after several accelerations for relatively large velocity ions. However, in the first gaps T_1, T_2, T_3 must be evaluated since the injection velocity in the gap of length g is still low. For an uniform electric field we have

$$T_1 = \frac{1}{E_0\, g}\int_{-g/2}^{+g/2} E_0\,\cos(\omega_{\text{rf}}\, t)\, ds = \frac{\sin(\frac{\omega_{\text{rf}}\, g)}{2\, v_0})}{\frac{\omega_{\text{rf}}\, g}{2\, v_0}} = \frac{\sin(\frac{H\, g}{2\, R_m})}{\frac{H\, g}{2\, R_m}},$$

using $t = \frac{s}{v_0}$, $\omega_{\text{rf}} = H\,\omega$ and $v_0 = R_m\,\omega$.
Therefore the curvature radii R_i after each acceleration are

$$R_1 = \frac{v}{\omega} = \frac{1}{\omega}\sqrt{\frac{2\, E_K 1}{m}} = \sqrt{R^2_m + T_1\,\frac{R^2_{\text{extraction}}}{N_{\text{turn}}\, N_{\text{gap}}}}$$

$R_2 = \sqrt{R_1^2 + T_2\,\frac{R^2_{\text{extraction}}}{N_{\text{turn}}\, N_{\text{gap}}}}$, $R_3 = \ldots$, $R_4 = \ldots$
Given the uniform field B_0, the trajectory is a series of half-circles. Knowing R_5,... , R_1 , we want to identify the ideal inflector position and the first rotation centre O_1 of the particle after injection. For that purpose,we draw a semi-circular trajectory centred at $O_5 = \Omega$, the cyclotron center,with a radius R_5. then, we go backward connecting half-circles with decreasing radii R_4,... R_1, to get the ideal position before the first acceleration. This determine the ideal location for the inflector exit. This guaranty that the beam rotation centres will converge toward the cyclotron centre Ω after 5 accelerations. (see Fig. I.13.18).

7.5 Radial injection for separated sector cyclotron

This technique is particular to separated sector cyclotron. This cyclotron kind is used to accelerate relatively high-energy ion beams. The injected beam comes from an accelerator and it is too rigid for a $B_\rho \geq 0.5\,\mathrm{Tm}$ to be injected axially with a compact electrostatic inflector like the hyperboloid inflector.

The separated sector cyclotrons (SSC) consist of magnet sectors separated by empty spaces (valleys), of a size that can fit an injection beam line. The radial injection beam line is made up from several magnets and at the end a high voltage electrostatic inflector, with two flat electrodes, provides the last kick to the injected beam without modifying the trajectory of the accelerated turns (one example is SSC2, Ganil, France, reproduced in Fig. I.13.21).

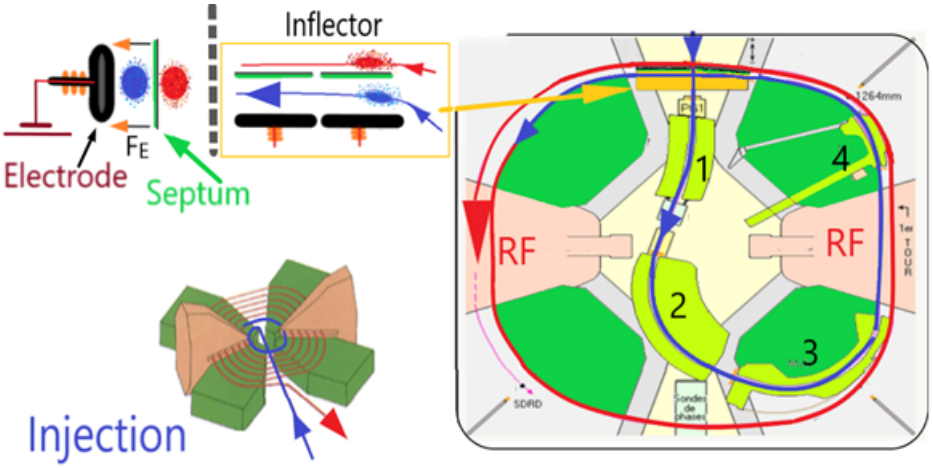

Fig. I.13.21: Radial injection of SSC2 (Ganil, France). The space available between the separated sector magnets of the SSC is used to insert the injection magnets (1,2,3,4) and an electrostatic inflector. The electrostatic inflector gives only a few milliradians deviation to align the beam with the accelerated orbit. The trajectory of the accelerated beam (in red) is not perturbed by the external electrode of the inflector which is at ground potential. The position of the electrostatic inflector can be moved to generate a precession, which can be helpful for the extraction (see also Section 8.2.2).

8 Extraction

The most frequently used extraction methods are stripping extraction and extraction by electrostatic deflectors [17, 18, 23].

8.1 Stripping extraction

Hydrogen isotopes (^{1}H or deuterium ^{2}H) can be produced in a negative ion state: i.e. a hydrogen atom can capture an extra-electron. Even if the extra-electron on an H^- ion is very loosely bound, we can accelerate these anions. After the acceleration, when passing through a thin carbon foil, the ion loses its electrons (by stripping). The thin carbon foil is positioned in the cyclotron magnetic field close to the extraction radius, the accelerated H^- ions by crossing the foil are transformed into H^+ ions. The change in the ion's sign changes the direction of the bending force (from $F_r = -e_0\, v_\theta B_z$ to $F_r = +e_0\, v_\theta B_z$),

and the positive ions are deviated toward the outside of the magnetic field. The stripping extraction techniques present many advantages and is very cost effective:

- The efficiency is closed to 100%, much better than with an electrostatic deflector;
- The foil lifetime even with large current is rather long ($\sim 10^4\,\mu$Ah);
- Simultaneous extraction of two beams toward two external lines is possible with two foils corresponding to beams of different energies and with different beam currents;
- A large energy range may be covered by changing the foil position in the magnetic field (correcting magnets are then needed to ensure a constant angle in the exit beam line);
- Negative ion source can provide H^- or negative deuterium D^- at high currents up to 0.5 mA (with an external multicusp source).

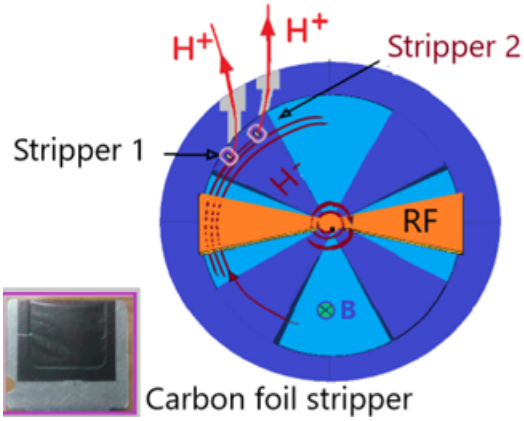

Fig. I.13.22: Stripping extraction for H^-. At the radius of the last orbit a thin carbon foil strips off the electrons. The residual ions are H^+ and the trajectories of the positive ions are bent in the opposite direction. The radial location of the stripper on the last orbit defines the beam energy. Several strippers can be inserted producing simultaneous beams. The simultaneously extracted beams are delivered to different applications at the same time, which is very cost effective. A picture of a carbon foil stripper is shown in the bottom left corner.

8.2 Deflector extraction: Single-turn extraction vs multi-turn extraction

For positive ions such as H^+ the stripping extraction is not possible and several optical elements must be used to bend the beam out of the cyclotron. The extraction hardware for a cyclotron usually consists of an electrostatic deflector followed by a magnetic channel. The curvature of the electrodes of the deflector must correspond to the shape of the orbits of the extracted ions. The deflector provides an angle kick of typically 50 mrad with an electric field of approximately $E = 100\,$kV/cm.

If the bunches are well separated radially (bunch size ΔR smaller than the turn separation δR), it is possible to adjust the acceleration voltage to direct most of the particles inside the electrostatic deflector without beam losses. One speaks then of single-turn extraction. If the bunches are not separated radially (size $\Delta R >$ turn separation δR), the bunch having performed N_{turn} turns overlaps the bunch on its $(N_{\text{turn}} - 1)$ turns, the deflector will cut a continuous stream of particles generating important beam

losses: in this case we talk about multi-turn extraction, which results in activation and HV sparking of the deflector. The reduction of beam losses in the deflector requires minimizing the beam size while maximizing the turn separation.

- Minimization of the bunch size ΔR: The minimization of the beam size Δr is obtained through transverse matching and longitudinal bunching.
  - Transverse matching: The cyclotron is a (quasi) periodic accelerator and the magnetic structure possesses an ideal periodic emittance in the transverse plane (the eigen ellipse). A mismatch between the cyclotron periodic ellipse and the injected beam will result in an increase of the beam emittance. It is always important to design the injection beam line to match properly the beam ellipse to the ideal periodic ellipse and to avoid emittance dilution, and getting the minimal bunch size at the extraction.
  - Longitudinal bunching: The energy dispersion can be reduced by a minimization of the phase width $\Delta\varphi = H\omega_{\text{rev}}\,\Delta t$ using a buncher, which results in a reduction of the bunch size

$$\frac{\Delta R}{R} = \frac{\Delta B\,\rho}{B\,\rho} = \frac{\Delta p}{p} = \frac{\gamma}{\gamma+1}\,\frac{\Delta E_k}{E_k} \approx \frac{1}{2}\,[\cos(0) - \cos(\frac{\Delta\varphi}{2})] \approx \frac{1}{4}\,\Delta\varphi^2 \quad . \text{(I.13.80)}$$

- Maximisation of the orbit separation δR: During acceleration the bunch spacing is reduced progressively $\delta R \sim 1/R$, the energy gain per turn being constant while the energy is increasing (see Eq. (I.13.19)). The conditions to obtain a single-turn extraction rely on the maximisation of the turn separation δR. Three techniques are used:
  - Maximal acceleration,
  - Precession,
  - Resonant extraction.

8.2.1 Acceleration for the maximisation of the turn separation

In high-energy isochronous cyclotron, the energy gain per turn can be increased by using more accelerating gaps: for example, the 8 separated sector cyclotron of PSI ($K_b = 590\,\text{MeV}$, see Fig. I.13.11), has four accelerating RF cavities located in the valleys. It provides 8 accelerating gaps. The number of valleys available restricts the number of the accelerating cavities. A bunch separation δR larger than 1 cm is rather difficult to obtain. Therefore, other additional mechanisms are required.

Exercise n^o10: Turn separation and energy gain per turn.

Demonstrate that the turn separation δR is dominated by the energy gain per turn δE_{turn} in the cyclotron, but is influenced as well by the average field index k

$$\frac{\delta R}{R} = \frac{\gamma}{\gamma+1}\frac{\delta E_{\text{turn}}}{E_N}\frac{1}{1+k}.$$

Answer:

Compute the radial gain δR per turn in a non-homogeneous field $\langle B\rangle \sim \langle R\rangle^k$.
Since

$$\frac{d\langle B\rangle}{dR} = \frac{d(R^k)}{dR} = kR^{k-1} = k\frac{\langle B\rangle}{R},$$

we have $\frac{\delta\langle B\rangle}{\langle B\rangle} = k\frac{\delta\langle R\rangle}{\langle R\rangle}$.
Besides, for a particle at a given orbit:

$$B\rho = \langle B\rangle\langle R\rangle \quad \text{so} \quad \langle R\rangle = \frac{B\rho}{\langle B\rangle},$$

$$\frac{\delta\langle R\rangle}{\langle R\rangle} = \delta\ln(\langle R\rangle) = \delta\ln\left(\frac{B\rho}{\langle B\rangle}\right) = \frac{\delta B\rho}{B\rho} - \frac{\delta\langle B\rangle}{\langle B\rangle} = \frac{\delta p}{p} + k\frac{\delta\langle R\rangle}{\langle R\rangle}.$$

This gives the acceleration + field variation over one turn. Rearranging δR on both sides:

$$\frac{\delta\langle R\rangle}{\langle R\rangle} = \left(\frac{\delta p}{p}\right)\frac{1}{1+k} = \left(\frac{\gamma}{\gamma+1}\frac{\delta E_{\text{turn}}}{E_N}\right)\frac{1}{1+k}.$$

(We have used: $\frac{dE_k}{E_k} = \frac{\gamma+1}{\gamma}\frac{dp}{p}$, see Appendix I.13.D).
The energy after N_{turn} is $E_N = E_{\text{injection}} + N_{\text{turn}}\delta E_{\text{turn}} \approx N_{\text{turn}}\delta E_{\text{turn}}$.
Therefore, the radial separation of two consecutive turns δR is:

$$\delta R = \langle R\rangle\frac{\gamma}{\gamma+1}\frac{\delta E_{\text{turn}}}{E_N}\frac{1}{1+k} \simeq \langle R\rangle\frac{\gamma}{\gamma+1}\frac{1}{N_{\text{turn}}}\frac{1}{Q_r^2}.$$

(We have seen that the radial tune is $Q_r^2 \simeq 1+k+\ldots$, see Section 4.5).
Consequently, for a desired cyclotron energy, if you have to increase the turn separation δR at the extraction in order to reduce the beam losses:

- Build cyclotrons with a large radius R;
- Make the energy gain per turn δE_{turn} as high as possible (it reduces N_{turn});
- Accelerate the beam into the fringing field, where $\langle B_z\rangle$ and Q_r^2 drop.

If the turn separation δR is not sufficient to obtain a single-turn extraction, we have to use precession and resonant extraction.

8.2.2 Precession

An orbital precession induced by an off-centering injection enhances the turn separation δR. Detuning slightly the beam at the cyclotron injection allows to shift the radial position by a few mm and, because of the betatron oscillation, the beam will oscillate with a frequency $(Q_r\,\omega t) \;=\; Q_r\,\theta$ (see Section 3). The position of a bunch after N revolutions at azimuth $\theta_1 \;=\; 2\pi\,N$ will be

$$R(\theta_1 \;= 2\pi\,N) \;=\; R_0\,(2\pi\,N) \;+\; x_N\,\cos(Q_r\,(2\pi\,N) \;+\; \varphi) \quad , \tag{I.13.81}$$

where the ideal orbit (without precession) after N turns is $R_0(\theta_1 \;=\; 2\pi\,N)$, is defined by the acceleration. The amplitude of the precession is given by the injection error x_0: $x_N \;=\; R_{0N}(\frac{x_0}{R_0})$. Since $Q_r \;\sim\; 1$ in an isochronous cyclotron, we can replace $\cos(Q_r\,(2\pi N)\,)$ by $\cos(\,(Q_r \;-\; 1)\,(2\pi N)\,)$. So, only the fractional part of the tune Q_r matters.

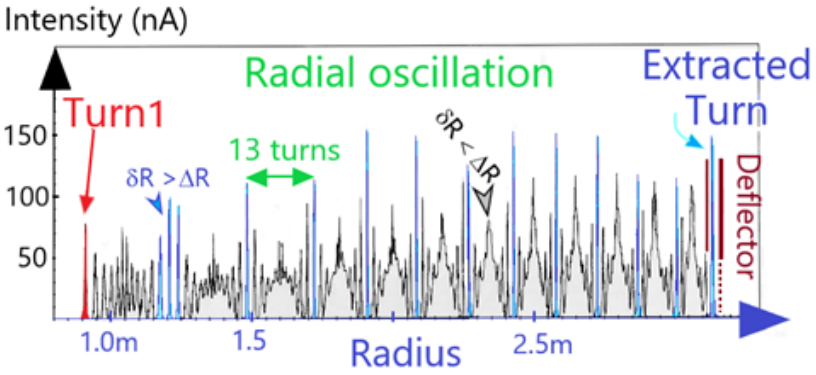

Fig. I.13.23: Precession by off-center injection. The beam intensity can be measured as a function of the cyclotron radius on a radial probe. This plot shows the intensity in the machine as a function of the orbit radius. For certain radii some orbits are so close that we cannot distinguish the different turns ($\delta\,R \;<\; \Delta\,R$), while for other radii, we see clearly different peaks when the turn separation is larger. These radial oscillations of the beam allow to increase the turn's separation $\delta\,R$ at the deflector for a single-turn extraction. For this cyclotron (Ganil SSC2), the precession is defined by the radial tune $(Q_r \;-\; 1) \;=\; \frac{1}{13}$ generating an apparent period of oscillation of 13 turns at the azimuth θ_1 of the measurement.

8.2.3 Resonant extraction

For a resonant extraction we generate an oscillation $x(\theta)$ close to the extraction point with some magnetic perturbations (field bumps). The radius of the trajectory will oscillate around a non-perturbed trajectory $R_0 :\; R(\theta) \;=\; R_0(\theta) \;+\; x(\theta)$.

Adding a magnetic perturbation at the extraction $\Delta B_z \;=\; B_P(R)\,\cos(P\theta)$, using $\theta = \omega\,t$, we get as in Section 3.3

$$\frac{d^2x}{d\theta^2} \;+\; Q_r^2\,x \;=\; A\,\cos(P\theta) \quad . \tag{I.13.82}$$

Note: a full derivation gives $A \;=\; (\frac{\langle R\rangle}{\langle B_z\rangle})\,(\frac{dB_P(R)}{dR})$.

This is the equation of a driven oscillator. We can try a particular solution $x(\theta) \sim \cos(P\theta)$ which gives the response function χ

$$\chi = \left[\frac{x(\theta)}{A}\right] = \frac{\cos(P\theta)}{(Q_r^2 - P^2)} \quad . \tag{I.13.83}$$

If the excitation frequency P corresponds to the natural frequency Q_r ($P \sim Q_r$), the response function $\chi = [\frac{x(\theta)}{A}]$ will diverge. This means, that a very small amplitude perturbation Δ induces a large amplitude motion $x(\theta) = \chi\,\Delta$. This is the definition of a resonance.

Note on resonances: Most of the time, in synchrotrons and cyclotrons, we try to adjust the tunes Q_z, Q_r to avoid resonances, by requiring $K\,Q_r + L\,Q_z \neq N$ during the acceleration, with K,L,N integers. For a resonant extraction, we excite on purpose the radial resonance ($K\,Q_r = N$), but only locally, close to the extraction radius to increase the turn separation δR.

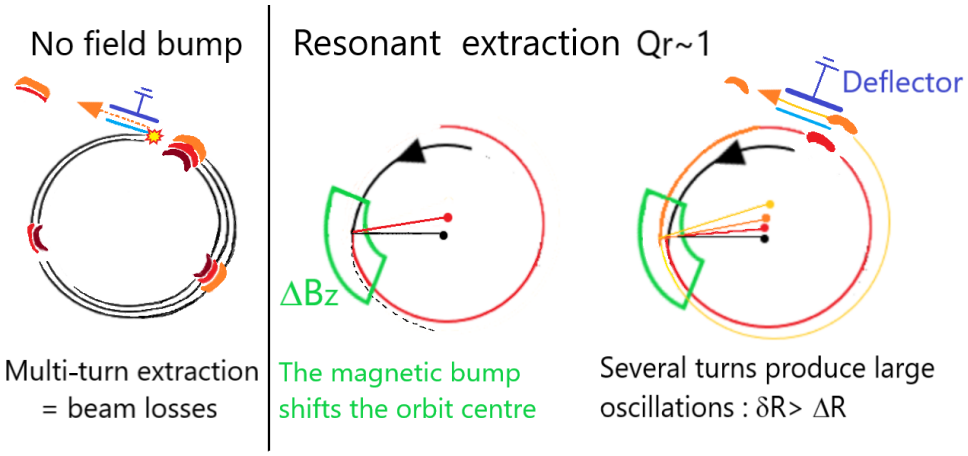

Fig. I.13.24: Principle of the excitation of the first order resonance using a magnetic bump. When $Q_r \sim 1$, a dipolar perturbation (ΔB_z) shifts the orbit centre at each turn. If the orbit separation is sufficient ($\delta R > \Delta R$), we can direct the full bunch through the extraction channel without beam losses thus obtaining a single-turn extraction.

In isochronous cyclotrons, the average field index is $k \sim \gamma^2 - 1$, so $Q_r^2 = 1 + k + \cdots = \gamma^2$ which defines the multi-polarities of the field perturbation to be used $P \sim \gamma$.

- For low energy cyclotron ($\gamma < 1.2$) a flat field bump localized at large radius with an aperture $\Delta\theta = 20\,\mathrm{deg}$ is sufficient mimicking a first harmonic perturbation $A\cos(\theta)$ and corresponds to a "$Q_r = 1$" resonance. This case $K = 1$ (low-order resonance) of the equation $K\,Q_r = N$, produces $N = 1$ oscillation per turn. Therefore, we excite the natural frequency with the perturbation from one side in the cyclotron and get the large amplitude motion on the other side.
- For higher energy cyclotrons ($\gamma < 1.5$) we can think to use $2\,Q_r = 3$. This "half-integer resonance" ($\frac{N}{K} = \frac{3}{2}$) can be excited with a magnetic quadrupole perturbation. Naturally, shifting a particle by a $\delta x = +1$mm from the reference trajectory at a given turn, becomes a negative shift $\delta x = \cos(3/2 \times 360°) = -1$ the next turn. The idea is to use a magnetic perturbation with gradient (a positive perturbation $\delta B = f(R_0 + x)$ at turn N, become $-\delta B = f(R_0 - x)$ at turn

$N + 1$) and will increase the amplitude of $|\delta x|$. This perturbation matches the natural periodicity of the beam over two turns:

$$\text{Natural oscillation } \delta x(N) = -\delta x\,(N+1) \quad \sim \quad \text{field bump } \delta B(N) = -\delta B\,(N+1) \quad .$$

– For proton synchrocyclotrons at 250 MeV ($\gamma = 1.26$) the idea of a quadrupolar perturbation is also applied. The magnetic perturbation, having a gradient, changes the focusing property and shifts the radial tune to a lower value $Q_r \sim 1$. We excite this resonance to mimic an ideal perturbation $\Delta B(R,\theta) = K\,(R - R_0)\cos(2\theta)$. This method is called "regenerative extraction". it required two perturbations: first, a negative quadrupolar perturbation (called "peeler") gives a radially outward impulse, then a positive quadrupolar perturbation (called "regenerator"), located $\sim 90\,^\circ$ apart, gives a radially inward impulse. The two radial kicks add constructively to increase the amplitude of a beam radial oscillation. The direction of the kicks depends of the particle radial position in the peeler and regenerator.

Table I.13.2: Overview of two resonances often used in cyclotron extraction.
For $Q_r = \frac{N}{K}$, the betatron oscillation corresponds to K oscillation periods within N turns.

Resonance $KQ_r = N$	Ideal perturbation	Field bump	Comments
$Q_r = 1$	$\cos(\theta)$	1 local dipolar perturbation: $\Delta B(\theta) = C_1\, f(\theta - \theta_0)$	Adapted to cyclotron with $Q_r \sim 1$ Energy selective effect
$2\,Q_r = 2$ $K = 2$ $N = 2$	$\cos(2\theta)$	"Regenerative extraction" 2 local gradients perturbations (quadrupolar fields) achieved with a neg. gradient + a pos. gradient located 90°apart. $\Delta B(R,\theta) =$ $-K(R-R_0)\,f(\theta - \theta_0) +$ $K(R-R_0)f(\theta - (\theta_0 + 90°))$	The quadrupole perturbation modify the field index k and radial tune. $Q_r^2 = 1 + k + \ldots$ If $k \sim -1$ (decreasing $\langle B \rangle$), δR increases exponentially since $\frac{\Delta R}{R} \sim \frac{1}{Q_r^2}$ -Radius selective effect -Useful for low energy gain per turn and bad beam quality (like in synchrocyclotrons).

9 Conclusion

The cyclotrons are cost effective hadron accelerators. The main application is the production of radioisotopes for medicine for diagnosis (imaging). The cancer therapy centres using 250 MeV proton cyclotron represents as well an application with an increasing interest. Besides, large cyclotrons are still used in many laboratories for research, and can accelerate various ions, even at very large beam power (a 1.4 MW proton beam has been obtained in PSI). We classify the cyclotrons as a function of their bending power K_b (we have $(E/A)_{\text{max}} = K_b(Q/A)^2$). The main formula, which drives all the concept of isochronism, is the particle revolution frequency in the cyclotron magnet

$$\omega_{\text{rev}} = \frac{q\,\langle B_z(R,\theta)\rangle_\theta}{m\,\gamma} \quad .$$

We have seen that several variations of the initial concept lead to 3 cyclotron kinds:

Isochronous cyclotrons the most diffused	**Synchrocyclotrons**	**FFAGs**
Particles: protons and ions	protons and ions	p, ions, electrons, muons
$F_{\text{rf}} = \text{constant} = HF_{\text{rev}}$ 100% duty cycle. CW	RF cycled ($F_{\text{rf}} \neq$ constant) typically $\sim 1\%$ duty cycle Faster cycling than a synchrotron	RF cycled ($F_{\text{rf}} \neq$ constant) typically$\sim 1\%$ duty cycle Faster cycling than a synchrotron
Azimuthal field modulations Rather complex magnets (AVF, SCC, spiral edge) Vertical foc. achieved mainly by edge focusing in the sectors	No azimuthal oscillations required Simpler magnet ($dB_z/dR < 0$) Vertical focusing comes from decreasing field	Azimuthal oscillations required Very complex magnet (alternate grad.,spiral edge) Vertical focusing comes from alternates gradients
Average field index $k(R) = \gamma^2 - 1$	k not constrained by isochronism	k not constrained by isochronism
Limited in energy $\gamma < 2$	Limited in energy $\gamma < 2$	Not limited in energy
Applications: radioisotope production, proton therapy, research in nuclear physics	Applications: proton therapy	Applications: proof of principle machines, accelerator driven system (?), future muon accelerator (?)

Acknowledgements I wish to thank specially F. Meot, E. Metral, J. Leduff, and F. Chautard, for enlightening comments on the present document. Many collaborators helped me to focus on a comprehensive text: M. Bozzo, O. Kamalou, M. Lalande.

Besides, many good lectures from other colleagues inspired the structure of this document (E. Baron, W. Kleeven and S. Zaremba , F. Chautard, M. Seidel). I'm indebted to the research laboratory working with cyclotrons and FFAGs for documents and pictures (PSI@Villigen, RIBF@Tokyo, GANIL@Caen, STFC@Daresbury). I thank warmly the IBA company for allowing me to reproduce the numerous pictures of commercial cyclotrons.

I.13.A The cyclotron CYCLONE® (IBA)

This accelerator is an industrial cyclotron for medical radioisotope production (^{18}F, ^{15}O, ^{11}C, ^{68}Ge, ^{123}I...) . For instance the Fluorine-18 is the most widely used radioisotope for imaging, it permits the positron emission tomography (PET) which is a powerful tool to detect cancerous tumors and metastases, and to monitor their evolution.

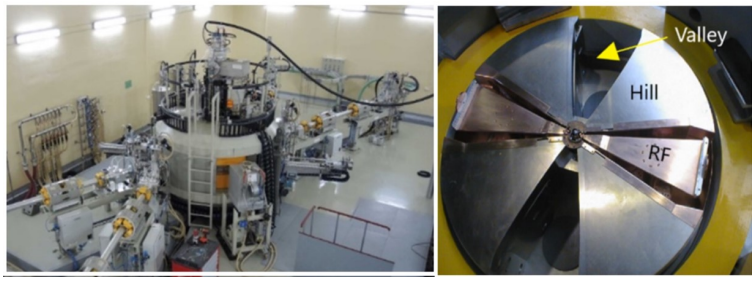

Fig. I.13.25: The CYCLONE 30 cyclotron.

It is a compact isochronous cyclotron with $K_b = 30\,\mathrm{MeV}$, and has four straight magnetic sectors. Azimuthally the magnetic field evolves from 1.7 T (in the hills) to 0.12 T (valleys) and two RF Dees are operated at $65\,\mathrm{MHz}$. The cyclotron delivers protons up to $30\,\mathrm{MeV}$, and deuterium and alpha particles up to $7.5\mathrm{MeV/A}$. The beam intensity can reach $800\,\mu\mathrm{A}$ for the proton beam.

This cyclotron is operated in 30 facilities in the world with low running costs (https://www.iba-radiopharmasolutions.com).

I.13.B The superconducting "Comet" at PSI for proton therapy

This accelerator is a $250\,\mathrm{MeV}$ proton compact cyclotron, and has been constructed by ACCEL for the Paul Sherrer Institute (PSI). The cyclotron delivers protons at fixed energy for cancer treatment. The cyclotron is a compact isochronous "Azimuthally Varying Field" with 4 spiral sectors. The superconducting coils, cooled by liquid helium, produce a field evolving from 3.8 T (hills) to 2.4 T (valleys). There are four accelerating RF Dees operated at 72 MHz ($H = 2$). The beam orbits 630 turns before extraction.

For treatments on the human body the beam energy is degraded with solid targets (carbon degraders) in order to deposit the maximal energy (corresponding to the "Bragg peak") at the right depth in the tumor.

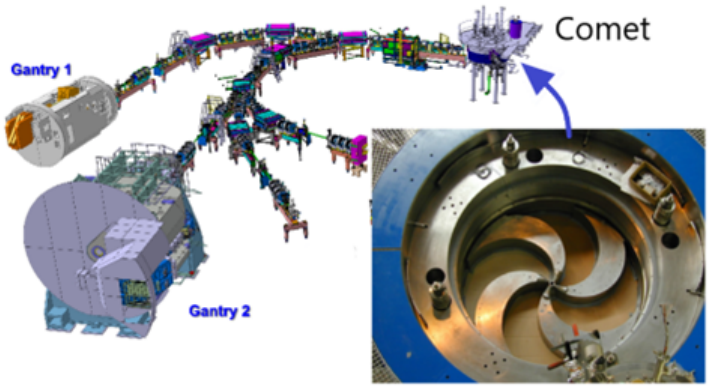

Fig. I.13.26: The COMET facility in PSI

The treatment station uses a rotating gantry to deposit the beam energy in the tumour with high precision, thus minimizing the damage to surrounding healthy tissues.

I.13.C RIBF facility (Tokyo, Japan)

The RIBF facility is built to produce rare radioactive nuclei for basic nuclear research, by the fission of energetic uranium ions. The accelerator facility uses a Linac and four isochronous cyclotrons in cascade. The largest cyclotron called SRC is a superconducting separated cyclotron with $K_b = 2600$ MeV (see Ex. 3). The SRC can boost the kinetic energy of an heavy ion beam at an energy which depends on the charge state Q and nucleon number A, $\frac{E_K}{A} = K_b\,(\frac{Q}{A})^2$. The ion source cannot provide fully stripped uranium ions with $Q = 92+$, but only $Q = 35+$. The uranium ions are stripped at two different energies with two strippers to obtain U^{86+} and to optimize the acceleration capability of the cyclotrons.

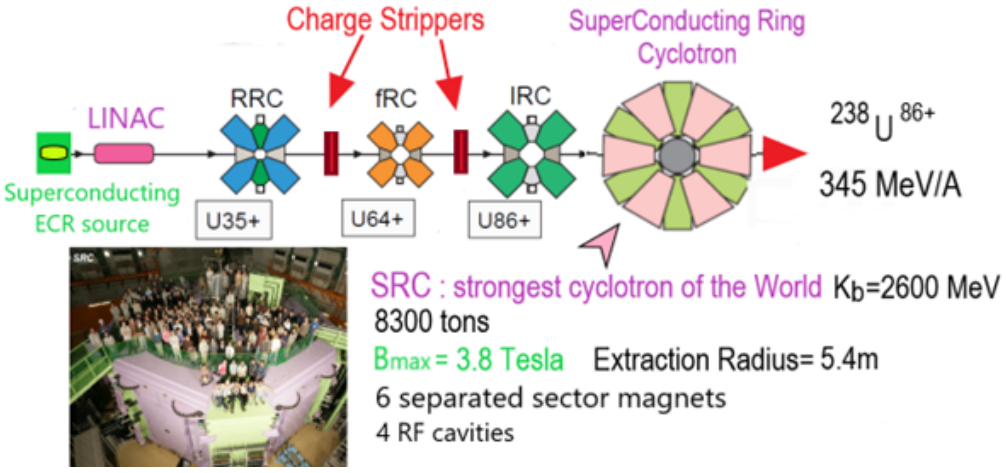

Fig. I.13.27: RIBF facility (Tokyo, Japan).

The coupling of two cyclotrons requires that the extraction velocity matches exactly the velocity of injection of the second cyclotron. Therefore, a strong constraint defines the matching of the RF harmonic and injection-extraction radii for the coupled cyclotrons.

For two consecutive coupled cyclotrons C1 and C2, we should have

$$v_{\text{injection C2}} = R\,\omega = \frac{2\pi\, R_{\text{injection C2}}\, F_{\text{RF2}}}{H_2} = v_{\text{extraction C1}} = \frac{2\pi\, R_{\text{extraction C1}}\, F_{\text{RF1}}}{H_1} \quad . \qquad \text{(I.13.84)}$$

Finally, the coupling of two cyclotrons requires

$$\frac{R_{\text{injection C2}}\, F_{\text{RF2}}}{H_2} = \frac{R_{\text{extraction C1}}\, F_{\text{RF1}}}{H_1} \quad . \qquad \text{(I.13.85)}$$

Besides, for the two respective RF frequencies we need $F_{\text{RF2}} = N\, F_{\text{RF1}}$ (N integer ≥ 1), in order to accept all the bunches in the cyclotron C2.

I.13.D Relativistic formulas

Some relativistic expressions are used in the lecture:

– The Lorentz factor $\gamma = \frac{1}{\sqrt{1-\beta^2}}$ with $\beta = v/c$,

- The total energy $E = \gamma mc^2 = \sqrt{p^2c^2 + m^2c^4}$,
- The rest energy $E_0 = mc^2$,
- The kinetic energy $E_k = E - E_0 = (\gamma - 1)mc^2$,
- The momentum $p = \gamma mv = \gamma m\beta c$,
- The particle magnetic rigidity $B\rho = \frac{p}{q} = \gamma\, m\beta c/q$.

We express generally the particle magnetic rigidity $B\rho = \frac{p}{q}$ in Tesla.meter (Tm). The magnetic rigidity permits an easy computation of the curvature radius in a transverse magnetic field B_0

$$\rho\,[m] = \frac{B\rho\,[Tm]}{B_0\,[T]}.$$

A useful relativistic relation is needed very often

$$(\beta\gamma)^2 = \frac{\beta^2}{1-\beta^2} = \frac{\beta^2 - 1 + 1}{1-\beta^2} = \gamma^2 - 1 = (\gamma+1)(\gamma-1).$$

Some derivatives are required, for instance in Ex. 10, to demonstrate that $\left(\frac{\Delta p}{p}\right) = \frac{\gamma}{\gamma+1}\left(\frac{\Delta E_k}{E_k}\right)$:

$$\frac{d\gamma}{d\beta} = \frac{d(1-\beta^2)^{-1/2}}{d\beta} = (-2\beta)\cdot\left(-\frac{1}{2}\right)\cdot(1-\beta^2)^{-3/2} = +\beta\gamma^3, \text{ therefore}$$

$$\frac{d\beta}{d\gamma} = \frac{1}{\beta\gamma^3},$$

$$\frac{dE_k}{d\beta} = \frac{d\left((\gamma-1)mc^2\right)}{d\beta} = mc^2\beta\gamma^3 = \frac{\gamma mc^2}{\beta}\beta^2\gamma^2 = \frac{\gamma mc^2}{\beta}(\gamma+1)(\gamma-1) = \frac{\gamma}{\beta}(\gamma+1)E_k,$$

$$\frac{dp}{d\beta} = mc\gamma + mc\beta\frac{d\gamma}{d\beta} = mc\gamma\left(1+(\beta\gamma)^2\right) = mc\gamma\left(1+(\gamma^2-1)\right) = mc\gamma^3.$$

Finally, using the last relations, we obtain

$$\frac{dE_k}{dp} = \left[\frac{d\beta}{dp}\right]\cdot\frac{dE_k}{d\beta} = \left[\frac{1}{mc\gamma^3}\right]\left[\frac{\gamma}{\beta}(\gamma+1)E_k\right] = \frac{(\gamma+1)}{\gamma}\left(\frac{E_k}{p}\right).$$

In the lecture, we used a consequence of the last formula in Secs. 12.2.5.3, 12.8.2, and Ex. 10

$$\frac{dE_k}{E_k} = \frac{(\gamma+1)}{\gamma}\left(\frac{dp}{p}\right).$$

References

[1] J.J. Livingood, *Principles of cyclic particle accelerators*, (Van Nostrand New York, NY, 1961), Internet Archive.

[2] M.K. Craddock, Physics & technology of cyclotrons & FFAGs, U.S Particle Accelerator School, 2010, https://uspas.fnal.gov/programs/2010/ucsc/courses/cyclotrons-ffags.shtml.

[3] W. Kleeven and S. Zaremba, Cyclotrons: Magnetic Design and Beam Dynamics, CAS 2015, doi:10.23730/CYRSP-2017-001.177.

[4] F. Chautard, Beam dynamics for cyclotrons, pres. European Cyclotron Progress Meeting ECPM XXXVIII, PSI, Villigen 9–12 May 2012, Indico PSI.

[5] M.S. Livingston, Part I, History of the cyclotron, *Phys. Today* **12** 10 (1959) 18–23, doi:10.1063/1.3060517; E.M. McMillan, Part II, History of the cyclotron, *ibid.*, 24–34 , doi:10.1063/1.3060517.

[6] AIEA, Database of cyclotrons for radionucleides productions, https://nucleus.iaea.org/sites/accelerators/Pages/Cyclotron.aspx.

[7] H.L. Hagedoorn and N.F. Verster, Orbits in an AVF cyclotron, *Nucl. Instrum. Meth.* **18–19** (1962) 201–228, doi:10.1016/S0029-554X(62)80032-9.

[8] M.M. Gordon and F. Marti, Electric focusing in cyclotrons with unusual dees, *Part. Accel.* **11** (1981) 161–172, CDS.

[9] P.K. Sigg, RF for cyclotrons, CAS 2005; doi:10.5170/CERN-2006-012.231.

[10] S. Zaremba, Magnets for cyclotrons, CAS 2005, doi:10.5170/CERN-2006-012.253.

[11] S. Machida, Fixed field alternating gradient, CERN Accelerator School 2011: High Power Hadron Machines, Bilbao, 2011, doi:10.5170/CERN-2013-001.33.

[12] M.K. Craddock, K.R. Symonn, Cyclotrons and fixed-field alternating-gradient accelerators, *Rev. Accel. Sci. Technol.*, **1** (2008) 65–97, 10.1142/9789812835215_0004.

[13] R. Edgecock *et al.*, 11th European Particle Accelerator Conference EPAC'08, Jun 2008, Genoa, Italy, pp. 3380–3382, JACoW.

[14] T. Ohkawa, Proceedings of annual meeting of JPS (1953).

[15] T. Planche *et al.*, Scaling FFAG rings for rapid acceleration of muon beams, *Nucl. Instrum. Meth. Phys. Res. A* **622** (2010) 21–27, doi:10.1016/j.nima.2010.06.242.

[16]] J. Van de Walle *et al.*, The S2C2: From Source to Extraction, in Proceedings of Cyclotrons 2016, Zurich, Switzerland, pp. 285–289, doi:10.18429/JACoW-Cyclotrons2016-THB01.

[17] P. Heikkinen, Injection and extraction for cyclotrons, CAS (1994), doi:10.5170/CERN-1994-001.819.

[18] W. Kleeven, Injection and extraction for cyclotrons, CAS (2004), doi:10.5170/CERN-2006-012.271.

[19] D. Toprek, Centering of the ion trajectory in the cyclotron, Nucl. Instrum. Meth. Phys. Res. A 480 (2002) 379–386, doi:10.1016/S0168-9002(01)01221-9.

[20] R.W. Müller, Novel inflectors for cyclic accelerators, *Nucl. Instrum. Meth.* **54** (1967) 29, doi:10.1016/S0029-554X(67)80004-1.

[21] J.L. Belmont, Ph.D. thesis, Grenoble, 1964; J.L. Belmont and J.L. Pabot, Study of Axial Injection for the Grenoble Cyclotron, *IEEE Trans. Nucl. Sci.* **13** 191–193, doi:10.1109/TNS.1966.4324204.

[22] D. Toprek, Theory of the paraxial ion trajectory in the spiral inflector, *Nucl. Instrum. Meth. Phys. Res. A* **449** (2000) 435–445, doi:10.1016/S0168-9002(00)00145-5.

[23] J.I.M. Boltman and H.L. Hagedoorn, Extraction from cyclotron, CAS (1994), CERN 94-01, Vol. II, pp. 169–185, doi:10.5170/CERN-1996-002.169.